Size and Structure of Spontaneously Forming Liposomes in Lipid/PEG-Lipid Mixtures

Montse Rovira-Bru, David H. Thompson, and Igal Szleifer
Purdue University, West Lafayette, Indiana 47907-1393 USA

ABSTRACT The optimal size and structure of spontaneous liposomes formed from lipid/polymer-lipid mixtures was calculated using a molecular mean-field theory. The equilibrium properties of the aggregate are obtained by expanding the free energy of a symmetric planar bilayer up to fourth order in curvature and composition of lipid and polymer. The expansion coefficients are obtained from a molecular theory that explicitly accounts for the conformational degrees of freedom of the hydrophobic tails of the lipid and of the polymer chains. The polar headgroup interactions are treated using the opposing forces model. The onset of stability of the symmetric planar film is obtained from the expansion up to quadratic order. For unstable planar films the equilibrium size and structure of the spherical aggregates is obtained from the second- and fourth-order terms in curvature and composition of lipid and polymer. The driving force for the formation of spontaneous vesicles is the asymmetric distribution of polymers between the inner and outer monolayer. The composition asymmetry between the two monolayers in the aggregates is much larger for the polymer component than for the lipid, and it depends upon the size of the aggregate. The smaller the aggregate, the more asymmetric the distribution of polymer and lipid. The tendency of the polymer chains to be tethered on the outer surface of the aggregate is very strong, and it limits the range of polymer loading for which spherical liposomes are stable. A very small excess of polymer loading causes small spherical micelles to be the optimal aggregates. In these cases spontaneous liposomes can form as metastable aggregates, showing as a local minima in the free energy. Even for metastable aggregates the asymmetric distribution of polymers is very large. The elastic constants of the asymmetric bilayer in the spherical aggregate are found to be the same as those that are calculated from the planar symmetric film. Therefore, the stable structure of the aggregate is not needed to determine its mechanical properties. The range of stable liposomes is very narrow in the range of molecular weights studied, which include the experimental relevant domain of aggregates used in drug delivery. It is found that the stability of the spherical aggregates results from a very fine balance between the tendency of the polymer chains and lipid tails to pack in an asymmetric spherical aggregate and the tendency of the hydrophobic-water interface to keep the area per molecule fixed. The changes in free energy per molecules that are responsible for liposome formation are very small and are very sensitive to detailed molecular properties. The theoretical description of the aggregates requires a theory capable of incorporating these detailed molecular properties. The findings are discussed in the context of vesicle formation and liposome design for drug delivery.

INTRODUCTION

The development of liposomes as drug carriers was facilitated in the early 1990s, when it was demonstrated that the inclusion of small percentages of lipid-bonded polymers (named polymer-lipids) in the liposome formulation increased its circulation time in vivo, favoring the uptake in the target site versus their elimination by the RES (Blume and Cevc, 1990; Allen et al., 1991). These liposomes are commonly referred to as stealth liposomes, and their resistance to blood stream elimination is due to steric stabilization by the polymer layer attached to the lipid bilayer (Klibanov et al., 1991; Needham et al., 1992; Torchilin et al., 1994a–c; Blume and Cevc, 1993). The most common polymer used for this purpose is poly(ethylene glycol) (PEG), also referred to as poly(ethylene oxide) (PEO). The effect of PEG in the stability of stealth liposomes has been extensively studied during the last decade. The protective effect of PEG layers is believed to prevent protein adsorption on the lipid bilayer (Ceh et al., 1997; Bradley et al., 1998) and, at the same time, to act as a steric barrier for inhibiting liposome fusion (Holland et al., 1996). As a result, successful lipid/PEG-lipid formulations have been developed for drug delivery. The amount of PEG in the formulations must be optimized, because too little PEG exhibits low protective effects in the bilayer, while too much PEG may lead to micellization of the system.

Most of the preparation procedures of PEG-stabilized liposomes reported in the literature involve nonreversible processes, such as dialysis, pH cycling, sonication, and extrusion. In contrast, there are few studies on spontaneous liposomes (Joannic et al., 1997; Szleifer et al., 1998). However, thermodynamically stabilized liposomes are expected to be more sensitive to environmental changes than kinetically trapped liposomes, which is a desirable property to explore for many uses in biological and pharmaceutical applications. Moreover, if the properties and behavior of spontaneous liposomes can be predicted with a model that includes the main features of a lipid/polymer-lipid bilayer, then one could control the state of the aggregate.

To determine the optimal characteristics of a liposome for experimental purposes, a quantitative theoretical approach

Submitted February 28, 2002, and accepted for publication June 27, 2002.
Address reprint requests to Igal Szleifer, Purdue University, Brown Bldg. 1393, West Lafayette, IN 47907-1393. Tel.: 765-494-5255; Fax: 765-494-5489; E-mail: igal@purdue.edu.

0006-3495/02/11/2419/21 $2.00

is needed to provide not only trends, but also comprehensive and practical guidelines. To meet this goal, we further investigate the origins and mechanisms of spontaneous PEG-stabilized liposome formation and the range of PEG-lipid compositions where liposomes form. Specifically, this study is focused on determining the conditions for energetically driven, isolated liposome formation. Energetically driven liposomes refer to those in which the free energy of the isolated aggregate in spherical geometry is lower than that of the planar bilayer. We devote special attention to understanding the molecular structure of the formed aggregates, which is often overlooked. Furthermore, the molecular driving forces for the formation of spontaneous liposomes, their range of stability, and the possible formation of small micellar aggregates is investigated.

The free energy of bilayers is usually described in terms of their elastic constants. Theoretical approaches are complex, because bending properties of these bilayers depend on the details of the molecular structure of the components and, for multicomponent formulations, their mutual interactions. The origin of spontaneous vesiculation was described by Safran et al. (1990) for bilayers of surfactants with identical hydrophobic regions but different polar groups. In this early study, it was shown that coupling between curvature and composition leads to vesicle formation when non-ideal mixing of surfactants occurs. Spontaneous vesicle formation was also predicted by Wang (1992) for a one-component bilayer composed of diblock copolymers. The composition of the diblocks must be sufficiently asymmetric with shorter chains in the core of the bilayer. Formation of polymer-based vesicles has been recently proven experimentally in water-containing solutions (Discher et al., 1999; Luo and Eisenberg, 2001) and in organic solvents (Ding and Liu, 1997). The formation of spontaneous vesicles was also predicted for mixtures of diblock copolymers (Dan and Safran, 1993). According to this study, the lamellar layer can be destabilized by the addition of small quantities of copolymers of different composition, with small fractions of shorter chains than the main component of the bilayer having stronger effects on the spontaneous curvature than a small fraction of longer chains.

The coupling between curvature and composition was further studied by Porte and Ligure (1995). Generalizing the ideas of Safran et al. (1990), they predicted a softening of the mean curvature modulus due to internal degrees of freedom when calculated at fixed chemical potential, which can lead to vesicle formation. Porte and Ligure (1995) extended their model to lipid bilayers having adsorbed polymer brushes, which they described in terms of a mean-field theory. Allowing the polymer to relax on both sides of the bilayer, they predicted that vesicle formation may occur at sufficiently high adsorption densities. However, the surface coverage they treated was much higher than the one commonly found in PEGylated liposomes for drug delivery. The effect of grafted polymer on the elastic constants of lipid bilayers has also been studied by Hristova and Needham (1994) and Marsh (2001), although none of them took into account the lipid/polymer-lipid relaxation. Those studies used scaling and mean-field theories to describe the polymer layer. These approaches are not expected to give quantitative predictions for low and moderate polymer coverage (Szleifer, 1996). Thus, they are not always applicable in the relevant experimental range of surface densities used in PEGylated liposomes.

Curvature-composition coupling has been shown to play a major role in the stability of bilayers and the resulting tendency to form spontaneous vesicles (Safran et al., 1990). However, there are no systematic studies that provide a deep understanding of the size and structure of thermodynamically stabilized aggregates formed as a result of that coupling. For this purpose, the application of a quantitative molecular theory to polymer-grafted liposomes is of great interest. A reliable theory would significantly reduce the experimental effort required to develop stable formulations with favorable biological and pharmacological properties. In addition, it would improve our understanding about how the molecular structure of the polymer and lipid layers determines the behavior of the layers.

In the present study, molecular mean-field (MMF) theory (Ben-Shaul et al., 1985; Szleifer and Carignano, 1996) is used to describe both lipid and PEG layers. MMF is applicable at experimentally relevant regimes of surface densities. Furthermore, the theory has been successfully used to provide quantitative predictions for several systems involving hydrocarbon tail packing in bilayer environments (Ben-Shaul et al., 1985) and PEG-grafted layers, such as adsorption isotherms of protein on PEG-grafted surfaces (McPherson et al., 1998; Satulovsky et al., 2000). MMF theory has also been applied to study the stability of PEGylated liposomes (Szleifer et al., 1998). In that study, the minimal loading of polymer necessary to destabilize planar bilayers was predicted as a function of polymer molecular weight. The predictions were successfully compared with experimental data. The limitation of that work, however, was that it only predicted the lack of stability of the planar film; the equilibrium size and structure of the spontaneous forming aggregates were not addressed. In the study presented here we extend that work. Our purpose is to predict not only the composition range where spontaneous liposomes form, but also the spontaneous curvature and the optimal structure of the aggregates.

In the next section we introduce our theoretical approach and a short description of the molecular theory used in this study. The following section introduces and discusses the results obtained. The last section presents the concluding remarks.

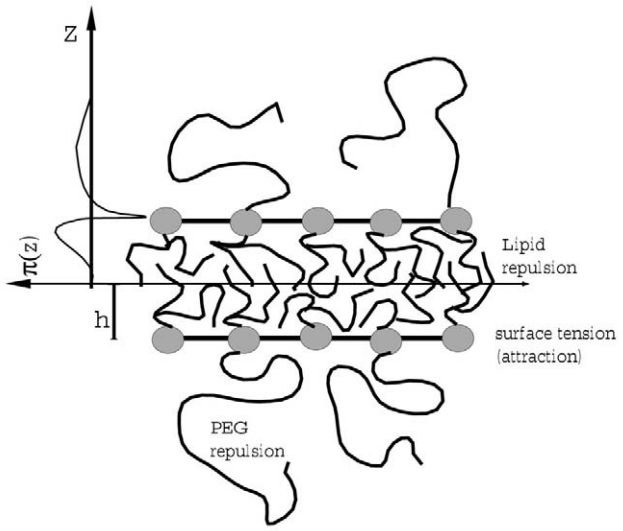

FIGURE 1 Schematic representation of a lipid/PEG-lipid bilayer. The qualitative shape of the stresses acting on the film is also represented. PEG, lipid tails, and lipid headgroups have a repulsive interaction (i.e., $\pi(z) > 0$), while the surface tension is the only attractive contribution ($\pi(z) < 0$).

MODEL

Free energy

The focus of this study is lipid/PEG-lipid bilayers. The lipid molecules are insoluble and have a double hydrocarbon chain tail that prefers the core of the bilayer to avoid contact with the surrounding water solution. The lipid tails are attached to a hydrophilic headgroup that lies on the water-lipid interface. A certain percentage of those headgroups are bonded to PEG chains that extend away from the interface toward the bulk solution. We assume that the lipid in the polymer-lipid molecule is the same as in the pure lipid. Fig. 1 shows a qualitative representation of the system.

In this study, we only consider the case of spherical liposomes of radius R. The aggregate is assumed to have a fixed number of lipids and polymer chains. We are interested in equilibrium aggregates. As a consequence, the only relevant case is that of free exchange of molecules across the bilayer, i.e., we assume that for all aggregates the chemical potential of the lipid molecules and the chemical potential of the PEG-lipid molecules are the same at both sides of the bilayer. The partition of the components between the two monolayers is expressed as $x_I = N_I^{out}/(N_I^{out} + N_I^{in})$, where I represents lipid or PEG molecules and N_I^{out} represents the number of I molecules in the outer monolayer of the bilayer. Thus, the relevant variables of the system are the partition of lipids and polymer-grafted chains between both sides of the membrane (x_{lipid} and x_{PEG}, respectively), together with the curvature ($c = 1/R$).

Based on Helfrich's seminal work (Helfrich, 1973), the classical description of the bending free energy for a symmetric bilayer expanded around the planar film ($c = 0$) contains terms on curvature up to quadratic order

$$\delta f = \frac{F(c, x_{lipid}, x_{PEG})}{A(0)} - \frac{F(0, \frac{1}{2}, \frac{1}{2})}{A(0)} = \frac{1}{2} Kc^2 \qquad (1)$$

where $F(c, x_{lipid}, x_{PEG})$ is the free energy of the aggregate at curvature c and lipid and PEG partition equal to x_{lipid} and x_{PEG}, respectively. $A(0)$ is the area at the surface of inextension, which corresponds to the area of the planar film. There are no linear terms in curvature because the expansion is made around the symmetric planar film. K corresponds to the second derivative of the free energy with respect to c, evaluated at $c = 0$. In terms of Helfrich's definition of the elastic constants we have $K = k_b + \bar{k}/2$, where k_b is the bending constant and $\bar{k}$ is the saddle-splay constant. In the cases of interest here, there is no need to define two independent elastic constants because we only treat spherical geometries. However, we mention their relations for completeness.

The free energy in Eq. 1 is expanded only as a function of c. The dependence of $F(c, x_{lipid}, x_{PEG})/A(0)$ with x_{lipid} and x_{PEG}, therefore, is included in K. Expanding the composition variables around the symmetric planar bilayer (i.e., $x_{lipid}^{planar} = x_{PEG}^{planar} = 1/2$) we have

$$(x_{lipid} - \tfrac{1}{2}) = \sum_i \frac{1}{i!} \left(\frac{d^i x_{lipid}}{dc^i} \right)_{c=0} c^i$$

$$(x_{PEG} - \tfrac{1}{2}) = \sum_i \frac{1}{i!} \left(\frac{d^i x_{PEG}}{dc^i} \right)_{c=0} c^i \qquad (2)$$

where $(d^i x_{lipid(PEG)}/dc^i)_{c=0}$ is the ith derivative of $x_{lipid(PEG)}$ with respect to c, evaluated at the planar geometry. For the case in which the lipid and polymer compositions can be varied independently, which are the only relevant cases as long as the percentage of PEGylated lipid is sufficiently low, the bending constant K is exactly given by (Ben-Shaul, 1995; Szleifer et al., 1998)

$$K = f_{c^2} + 2f_{c,x_{lipid}}\eta_{lipid} + 2f_{c,x_{PEG}}\eta_{PEG} + f_{x_{lipid}^2}\eta_{lipid}^2 + f_{x_{lipid}^2}\eta_{PEG}^2 \qquad (3)$$

where $f_{I^2} = d^2\delta f/dI^2$ and $f_{I,J} = d^2\delta f/dIdJ$, while $\eta_{lipid} = dx_{lipid}/dc$ and $\eta_{PEG} = dx_{PEG}/dc$. Thus, the elastic constant depends only on the first-order derivative of the composition variables with curvature. For the mixture in equilibrium, η_{lipid} and η_{PEG} are the ones that minimize K and hence the free energy, i.e., $\eta_{lipid} = (f_{c,x_{lipid}}/f_{x_{lipid}^2}^2)$ and $\eta_{PEG} = -(f_{c,x_{PEG}}/f_{x_{PEG}^2}^2)$.

When $K > 0$ the free energy is minimum for planar symmetric bilayers. Thus, the lamellar phase is the energetically preferred structure. In those cases, giant liposomes may form due to edge effects or favorable entropic contributions, but only for $0 \leq K \approx 1$. However, the formation of other lipid aggregates such as liposomes or micelles is favored at $K < 0$. In those cases, the planar bilayer correspond to a maximum in the free energy. The reduction of the free energy upon formation of a spherical aggregate arises from the coupling between the composition and the curvature, namely, the ability of the molecules to change the ratio between the two monolayers is responsible for the change in sign of K. The problem, however, is that no optimal size and/or structural information of the aggregates can be obtained from the second-order expansion.

Our previous calculations (Szleifer et al., 1998) concentrated on looking at the conditions upon which the elastic constant changes sign. Here we are also interested in predicting what is the optimal size and structure of the spherical aggregates that form when $K < 0$. To this end, we could follow two different routes. One is to calculate the free energy of the aggregates at all curvatures and compositions for a fixed number of lipids and PEGylated lipids. This is an almost impossible task because it requires the variation of three variables simultaneously. The second way is to continue the free energy expansion along the lines used for the quadratic expression. An expansion to fourth order should provide the optimal aggregate properties for the cases that $K < 0$. Thus, we could write

$$\delta f = \frac{F(c, x_{lipid}, x_{PEG})}{A(0)} - \frac{F(0, \frac{1}{2}, \frac{1}{2})}{A(0)}$$

$$= \tfrac{1}{2} Kc^2 + \tfrac{1}{24} \lambda c^4 \qquad (4)$$

where there are no third-order terms because we are expanding around the planar symmetric film. As for the second-order expansion, Eq. 4 is ex-

pressed only in terms of curvature. Therefore, composition-curvature coupling is implicitly included in K and λ. The coupling between composition and curvature in λ goes beyond the linear term coefficients that are needed for K. Actually, one needs terms up to third order in the expansions presented in Eq. 2. The minimization of the free energy will not enable the determination of all the necessary coefficients and, therefore, it is more convenient to directly expand the free energy up to fourth order in curvature, c, and lipid and polymer composition, $x_{\text{lipid(PEG)}}$, the three variables of the system.

The free energy of the lipid/polymer-lipid mixture up to fourth order is given by

$$\begin{aligned}\delta f &= \frac{F(c, x_{\text{lipid}}, x_{\text{PEG}}) - F(0, \frac{1}{2}, \frac{1}{2})}{A(0)} \\ &= \tfrac{1}{2} f_{c^2} c^2 + \tfrac{1}{2} f_{x^2_{\text{lipid}}} (x_{\text{lipid}} - \tfrac{1}{2})^2 + \tfrac{1}{2} f_{x^2_{\text{PEG}}} (x_{\text{PEG}} - \tfrac{1}{2})^2 \\ &\quad + f_{c,x_{\text{lipid}}} c (x_{\text{lipid}} - \tfrac{1}{2}) + f_{c,x_{\text{PEG}}} c (x_{\text{PEG}} - \tfrac{1}{2}) \\ &\quad + \tfrac{1}{6} f_{c,x^3_{\text{lipid}}} c (x_{\text{lipid}} - \tfrac{1}{2})^3 + \tfrac{1}{6} f_{c,x^3_{\text{PEG}}} c (x_{\text{PEG}} - \tfrac{1}{2})^3 \\ &\quad + \tfrac{1}{4} f_{c^2,x^2_{\text{lipid}}} c^2 (x_{\text{lipid}} - \tfrac{1}{2})^2 + \tfrac{1}{4} f_{c^2,x^2_{\text{PEG}}} c^2 (x_{\text{PEG}} - \tfrac{1}{2})^2 \\ &\quad + \tfrac{1}{6} f_{c^3,x_{\text{lipid}}} c^3 (x_{\text{lipid}} - \tfrac{1}{2}) + \tfrac{1}{6} f_{c^3,x_{\text{PEG}}} c^3 (x_{\text{PEG}} - \tfrac{1}{2}) \\ &\quad + \tfrac{1}{24} f_{c^4} c^4 + \tfrac{1}{24} f_{x^4_{\text{lipid}}} (x_{\text{lipid}} - \tfrac{1}{2})^4 + \tfrac{1}{24} f_{x^4_{\text{PEG}}} (x_{\text{PEG}} - \tfrac{1}{2})^4 \end{aligned} \tag{5}$$

where $f_{I^i} = \partial^i \delta f / \partial I^i$ and $f_{I^i,J^j} = \partial^{i+j} f / \partial I^i \partial J^j$, with all the derivatives evaluated at the expansion point, i.e., $c = 0$; $x_{\text{lipid}} = x_{\text{PEG}} = 1/2$. Thus, the determination of the expansion coefficients will allow for finding the optimal size and molecular partition of the aggregates.

The strategy to find the optimal liposomes is the following. First, we use the expansion only up to second order, as given in Eq. 1, to determine the minimum total loading of polymer necessary to have $K < 0$ for each polymer molecular weight. Second, for loadings where spontaneous liposome formation is predicted, we use Eq. 5 to find the optimal aggregate size and structure. Namely, we find the curvature and composition asymmetry of lipids and polymer that minimize the free energy.

Two comments should be made at this point. First, the free energy expansions used up to this point assume that the area per molecule at which the molecules are packed is known and does not change upon bending. We will determine this area by minimizing the free energy of the planar film, from which the expansion is made, with respect to the area per lipid molecule, $a(0)$. Details are given below. Second, we are only describing the optimal size of an isolated aggregate. However, one would expect to have a complete size distribution of aggregates. The full determination of the size distribution can be obtained from the full free energy; however, it is beyond the scope of the work presented here.

The next step is the determination of the phenomenological expansion coefficients from a molecular approach. We apply a molecular theory to describe the lipid tails and PEG chains. This theory has been shown to be successful in describing the properties of lipid tails and PEG chains for conformational and thermodynamic properties. We formulate the free energy of the system based on this molecular theory. We differentiate this microscopic free energy with respect to curvature and composition of lipids and polymers. This provides the coefficients that are needed in the phenomenological expansion, Eq. 5. The main advantage of this method is that we can determine all the coefficients using the molecular theory applied only to the symmetric planar film. This is a very efficient way to perform systematic calculations that could not be done if the explicit free energy as a function of c, x_{lipid}, and x_{PEG}, needed to be determined for each combination of variables.

We consider that the hydrophilic heads of the lipids are located at the lipid-solvent interface. It is assumed that an a priori determined percentage of the total number of lipid heads are covalently attached to PEG chains. The hydrophobic lipid tails form a continuous isolated phase, i.e., no penetration of solvent and/or PEG chains into the hydrophobic phase is allowed. Fig. 1 shows a schematic representation of the system.

Both hydrophobic tails and polymer-grafted chains are described using MMF theory. The headgroup interactions will be modeled using the opposing forces approach of Tanford (Israelachvili, 1991). A detailed description of MMF can be found elsewhere for the lipid tails (Szleifer et al., 1990; Ben-Shaul, 1995) and for grafted polymer chains (Szleifer and Carignano, 1996). A basic description of the relevant aspects of the MMF model for our system is provided below. The basic idea of the theory is to look at a central chain with its intramolecular interactions taken into account in an exact way, within the chosen molecular model, while the intermolecular interactions are considered within a mean-field approximation. Due to the inhomogeneous character of the system in the direction perpendicular to the interface, z, the mean-field felt by the molecules is inhomogeneous in that direction. We show below a short derivation for the lipid chains and for the polymers. The difference arises from the fact that the hydrophobic lipid tails are assumed to be in a melt (no solvent) environment, while the polymer chains share the volume with the solvent molecules.

The starting point of the theory is to write the free energy of the system in terms of the probability distribution function (pdf) of chain conformations of the polymer (or lipid tails) and the distribution of solvent (absent for the lipid case). Thus, for the polymer case the free energy can be expressed as

$$\begin{aligned}\beta F_{\text{PEG}} &= N^{\text{in}}_{\text{PEG}} \sum_{\alpha} P^{\text{in}}_{\text{PEG}}(\alpha)[\ln[P^{\text{in}}_{\text{PEG}}(\alpha)] + \varepsilon^{\text{in}}_{\text{PEG}}(\alpha)] \\ &\quad + N^{\text{in}}_{\text{PEG}} \ln[\sigma^{\text{in}}/\sigma] \\ &\quad + \int_{-\infty}^{-h} N_{\text{solvent}}(z) \ln[N_{\text{solvent}}(z)] G(z) dz \\ &\quad + N^{\text{out}}_{\text{PEG}} \sum_{\alpha} P^{\text{out}}_{\text{PEG}}(\alpha)[\ln[P^{\text{out}}_{\text{PEG}}(\alpha)] + \varepsilon^{\text{out}}_{\text{PEG}}(\alpha)] \\ &\quad + N^{\text{out}}_{\text{PEG}} \ln[\sigma^{\text{out}}/\sigma] \\ &\quad + \int_{h}^{\infty} N_{\text{solvent}}(z) \ln[N_{\text{solvent}}(z)] G(z) dz \end{aligned} \tag{6}$$

where z denotes the radial distance from the bilayer midplane and $G(z)$ is a geometric factor that is unity for planar films and is the spherical element of volume for the spherical aggregates. N^i_{PEG} is the number of PEG chains grafted at the interface i = in (out), $P^i(\alpha)$ is the probability for the PEG chain to be in conformation α, $\varepsilon^{\text{in(out)}}_{\text{PEG}}(\alpha)$ is the internal energy of the PEG chain in the inner (outer) interface in that conformation, σ^i is the number of chains per unit area at interface i; σ is the chain surface density of the planar symmetric bilayer, and $N_{\text{solvent}}(z)$ is the number of solvent molecules at z. The first and fourth terms in Eq. 6 account for the conformational entropy of the PEG-grafted chains, while the second and fifth terms describe the translational entropy of the polymer at each monolayer of the bilayer. The third and sixth terms are the z-dependent translational entropy of the solvent. Note that $P^i_{\text{PEG}}(\alpha)$, N^i_{PEG}, $N_{\text{solvent}}(z)$, and σ^i are all functions of the curvature.

The free energy of the lipid tails, F_{lipid}, is given by

$$\beta F_{\text{lipid}} = N^{\text{in}}_{\text{lipid}} \sum_{\alpha'} P^{\text{in}}_{\text{lipid}}(\alpha')\ln\{[P^{\text{in}}_{\text{lipid}}(\alpha')] + \beta\varepsilon^{\text{in}}_{\text{intra}}(\alpha')\} + N^{\text{out}}_{\text{lipid}} \sum_{\alpha'} P^{\text{out}}_{\text{lipid}}(\alpha')\{\ln[P^{\text{out}}_{\text{lipid}}(\alpha')] + \beta\varepsilon^{\text{out}}_{\text{intra}}(\alpha')\} + N^{\text{in}}_{\text{lipid}}\ln[\sigma^{\text{in}}_{\text{lipid}}/\sigma_{\text{lipid}}] + N^{\text{out}}_{\text{lipid}}\ln[\sigma^{\text{out}}_{\text{lipid}}/\sigma_{\text{lipid}}] \quad (7)$$

which includes the conformational entropy of the chains and the internal energy of the molecules, with $\varepsilon^{\text{in(out)}}_{\text{intra}}(\alpha')$ being the internal energy of a chain in the inner (outer) monolayer in conformation α'. The last two terms correspond to the translational entropy of the molecules. There are only terms for the lipid chains because the hydrophobic core of the bilayer is assumed to be dry, i.e., without any solvent.

The repulsive intermolecular interactions are included in the model as hard-core excluded volume. These interactions are accounted for by packing constraints, which assume that the total volume available at each layer parallel (concentric) to the bilayer midplane (which is the origin of the z axis) must be filled with PEG segments or solvent for the polymer layer or with lipid tail segments for the hydrophobic core of the lipid bilayer. They are expressed as

$$N^{\text{in}}_{\text{PEG}} \sum_{\alpha} P^{\text{in}}_{\text{PEG}}(\alpha)n^{\text{in}}_{\text{PEG}}(\alpha, z)v_{\text{PEG}}dz + N_{\text{solvent}}(z)v_{\text{solvent}}dz = A(z)dz \quad -\infty \le z \le -h$$

$$N^{\text{out}}_{\text{PEG}} \sum_{\alpha} P^{\text{out}}_{\text{PEG}}(\alpha)n^{\text{out}}_{\text{PEG}}(\alpha, z)v_{\text{PEG}}dz + N_{\text{solvent}}(z)v_{\text{solvent}}dz = A(z)dz \quad h \le z \le \infty$$

$$N^{\text{in}}_{\text{lipid}} \sum_{\alpha'} P^{\text{in}}_{\text{lipid}}(\alpha')n^{\text{in}}_{\text{lipid}}(\alpha', z)v_{\text{lipid}}dz + N^{\text{out}}_{\text{lipid}} \sum_{\alpha'} P^{\text{out}}_{\text{lipid}}(\alpha')n^{\text{out}}_{\text{lipid}}(\alpha', z)v_{\text{lipid}}dz = A(z)dz \quad -h < z < h \quad (8)$$

where $A(z) = A(0)(1 + 2cz + c^2z^2)$ is the total area at distance z from the bilayer midplane, v_{PEG} is the volume of a PEG segments, v_{solvent} is the volume of the solvent, v_{lipid} is the volume of a lipid segment, and $n^{\text{i}}_{\text{lipid(PEG)}}(\alpha, z)$ is the number of chain segments in z at conformation α. For simplicity, we assume that $v_{\text{solvent}} = v_{\text{PEG}} = v$.

$P^{\text{in}}_{\text{PEG}}(\alpha)$, $P^{\text{out}}_{\text{PEG}}(\alpha)$, $P_{\text{lipid}}(\alpha')$, and $N_{\text{solvent}}(z)$ are determined by minimizing the free energy (Eq. 6 for grafted PEG and Eq. 7 for lipid tails) subject to the packing constraints (Eqs. 8). The minimization is carried out by introducing a set of Lagrange multipliers, $\beta\pi_{\text{lipid}}(z)$ in the lipid region and $\beta\pi_{\text{PEG}}(z)$ in the polymer-solvent region. The results are

$$P^{\text{in}}_{\text{lipid}}(\alpha') = \frac{\exp(-\beta\varepsilon_{\text{intra}}(\alpha') - \int_{-\text{h}}^{\text{h}} \beta\pi_{\text{lipid}}(z)v_{\text{lipid}}n^{\text{in}}(\alpha', z)dz)}{Q^{\text{in}}_{\text{lipid}}}$$

$$P^{\text{out}}_{\text{lipid}}(\alpha') = \frac{\exp(-\beta\varepsilon_{\text{intra}}(\alpha') - \int_{-\text{h}}^{\text{h}} \beta\pi_{\text{lipid}}(z)v_{\text{lipid}}n^{\text{out}}(\alpha', z)dz}{Q^{\text{out}}_{\text{lipid}}}$$

$$P^{\text{in}}_{\text{PEG}}(\alpha) = \frac{\exp(-\beta\varepsilon_{\text{intra}}(\alpha') - \int_{-\infty}^{-\text{h}} \beta\pi^{\text{in}}_{\text{PEG}}(z)vn^{\text{in}}(\alpha, z)dz}{Q^{\text{in}}_{\text{PEG}}}$$

$$P^{\text{out}}_{\text{PEG}}(\alpha) = \frac{\exp(-\beta\varepsilon_{\text{intra}}(\alpha) - \int_{\text{h}}^{\infty} \beta\pi^{\text{out}}_{\text{PEG}}(z)vn^{\text{out}}(\alpha, z)dz}{Q^{\text{out}}_{\text{PEG}}}$$

$$N_{\text{solvent}}(z) = \frac{A(z)}{v}\exp(-\beta\pi_{\text{PEG}}(z)v) \quad (9)$$

$Q^{\text{i}}_{\text{lipid}} = \Sigma_{\alpha'} \exp(-\beta\varepsilon_{\text{intra}}(\alpha') - \int_{-\text{h}}^{\text{h}} \beta\pi_{\text{lipid}}(z)v_{\text{lipid}}n^{\text{i}}(\alpha', z)dz)$ is the partition function (normalization constant) of the lipid in monolayer i. $Q^{\text{i}}_{\text{PEG}} = \Sigma_{\alpha} \exp(-\beta\varepsilon_{\text{intra}}(\alpha) - \int_{\text{h}}^{\infty} \beta\pi^{\text{i}}_{\text{PEG}}(z)vn^{\text{i}}(\alpha, z)dz$ is the partition function (normalization constant) of the PEG molecules attached to interface i. $\pi_{\text{lipid}}(z)$ and $\pi_{\text{PEG}}(z)$ are the lateral pressures acting on the central chain at each z to fulfill the packing constraints. The magnitudes of $\pi_{\text{lipid}}(z)$ and $\pi_{\text{PEG}}(z)$ indicate the level of compression of the chains at each distance from the center of the bilayer. A thorough discussion of the physical origin of the Lagrange multipliers can be found in Ben-Shaul et al. (1985) and Szleifer and Carignano (1996).

The values of the Lagrange multipliers are obtained by replacing the explicit expressions for the pdfs and the solvent distribution, Eqs. 9, into the constraint equations, Eqs. 8. The input necessary to solve the equations is $A(z)$ for all z, the set of single chain configurations for the PEG and the set for the lipid chains, the surface coverage of polymer and the thickness of the bilayer, $2h$. Then, the equations are solved by standard numerical methodologies from which the lateral pressures are obtained, and from them any desired average conformational and thermodynamic property of the aggregate. A detailed description can be found in Szleifer and Carignano (1996).

Introducing the explicit forms of the pdfs and solvent distribution, Eqs. 9, into the free energy for the PEG, Eq. 6, we obtain

$$\beta F_{\text{PEG}} = -N^{\text{in}}_{\text{PEG}}\ln Q^{\text{in}}_{\text{PEG}} + N^{\text{in}}_{\text{PEG}}\ln[\sigma^{\text{in}}/\sigma] - \int_{-\infty}^{-\text{h}} \beta\pi_{\text{PEG}}(z)A(z)dz - N^{\text{out}}_{\text{PEG}}\ln Q^{\text{out}}_{\text{PEG}} + N^{\text{out}}_{\text{PEG}}\ln[\sigma^{\text{out}}/\sigma] - \int_{\text{h}}^{\infty} \beta\pi_{\text{PEG}}(z)A(z)dz \quad (10)$$

and for the lipid, Eq. 7, we get

$$\beta F_{\text{lipid}} = -N^{\text{in}}_{\text{lipid}}\ln Q^{\text{in}}_{\text{lipid}} + N^{\text{in}}_{\text{lipid}}\ln[\sigma^{\text{in}}/\sigma] - \int_{-\text{h}}^{\text{h}} \beta\pi_{\text{lipid}}(z)A(z)dz - N^{\text{out}}_{\text{lipid}}\ln Q^{\text{out}}_{\text{lipid}} + N^{\text{out}}_{\text{lipid}}\ln[\sigma^{\text{out}}/\sigma] \quad (11)$$

Note that the geometry of the aggregate enters to the PEG and lipid chain free energies through the lateral pressures, $\pi_{\text{lipid(PEG)}}(z)$, and the area, $A(z)$.

The last remaining element is the treatment of the lipid headgroups. We use the opposing forces model of Tanford (Israelachvili, 1991), in which there are attractive interactions arising from the hydrocarbon-water surface tension and a repulsive term that accounts, in an approximate way, for the steric interactions between the headgroups. There are two contributions arising from the two interfaces that give

$$F_{\text{heads}} = \gamma A(-h)\left(1 + \frac{A_{\text{h}}^2}{A^2(-h)}\right) + \gamma A(h)\left(1 + \frac{A_{\text{h}}^2}{A^2(h)}\right) \quad (12)$$

where γ is the hydrocarbon-water surface tension and A_h is a phenomenological parameter that measures the strength of the repulsions between the headgroups.

The total free energy of the system is obtained by adding the three contributions from Eqs. 10–12. It turns out to be more convenient to define the free energy per lipid molecule, given by

$$f_{total}(a(0), c, r_{PEG}, x_{lipid}, x_{PEG}) = f_{PEG} + f_{lipid} + f_{heads} = \frac{F_{PEG}}{N_{lipid}} + \frac{F_{lipid}}{N_{lipid}} + \frac{F_{heads}}{N_{lipid}} \quad (13)$$

with $N_{lipid(PEG)} = N^{in}_{lipid(PEG)} + N^{out}_{lipid(PEG)}$. The total free energy is a function of the area per lipid molecule, $a(0) = A(0)/N_{lipid}$, the curvature, c, the ratio of PEGylated lipid molecules, $r_{PEG} = N_{PEG}/N_{lipid}$, the asymmetry of the lipids, $x_{lipid} = N^{out}_{lipid}/N_{lipid}$, and the asymmetry of the polymer chains, $x_{PEG} = N^{out}_{PEG}/N_{PEG}$. The phenomenological expansion of the free energy in Eq. 5 does not include the area. The reason is that we are assuming that the area per (lipid) molecule does not change upon deformation. That area is the surface of inextension, which for a symmetric planar bilayer is the midplane. Thus, the area $a(0)$ is kept constant upon the formation of spherical liposomes.

The value of $a(0)$ that we use is the one that minimizes the free energy of the planar bilayer. Namely, for each type of lipid molecule and each loading of polymer the total free energy is minimized with respect to area. The area at the minimum is the $a(0)$ that we use throughout the calculations for that lipid and polymer loading. The area per molecule that minimizes the free energy of the aggregate is the correct one to use because we assume that the lipids are insoluble in the solvent. Therefore, all the lipid molecules are involved in aggregate formation. Note that in the case of soluble lipids (or surfactants), the area per molecule is not determined by minimizing the free energy of the aggregate with respect to area. Rather, the optimal area is the one in which the lipids have the same chemical potential as those found dissolved in the solvent. However, as mentioned above we are only interested here in insoluble lipids.

One of the interesting results in insoluble lipids is that because the proper packing is the one in which the area per molecule is the one that minimizes the free energy, the bilayer is therefore a tensionless aggregate. Namely, the stresses acting on the bilayer must cancel. This implies strong restrictions on the number of PEGylated lipids that can be included in the aggregate, because the only attractive interaction in the bilayer is the fixed water-oil surface tension. This interaction must balance exactly the repulsions arising from the packing of the lipid tails, the lipid headgroups, and the polymers.

The balance of forces can be seen in more detail by minimizing the free energy, Eq. 13, with respect to the area. In other words, we need to find the area for which

$$\frac{\partial f_{total}}{\partial a} = 0$$

which gives

$$\gamma\left(1 - \frac{a_h^2}{a^2(0)}\right) - \int [\beta\pi_{lipid}(z) + \Pi_{PEG}(z)]dz = 0 \quad (14)$$

where $\Pi_{PEG}(z) = (1 - \exp(-\beta\pi_{PEG}(z)v - \beta\pi_{PEG}(z)v)/v$ is the lateral pressure of the polymer-solvent layer (Szleifer and Carignano, 1996). To understand the balance of forces let us take the case in which $a_h = 0$. Namely, the repulsive contribution of the lipid headgroups is zero. Actually, this is usually the case because $a_h \ll a(0)$ and, thus, it gives only a minor contribution to the repulsion. In this case, the equilibrium area of the bilayer is determined by the equality

$$\gamma = \int [\pi_{lipid}(z) + \Pi_{PEG}(z)]dz. \quad (15)$$

Both $\pi_{lipid}(z)$ and $\Pi_{PEG}(z)$ are absolute positive quantities because they represent the pressure arising from the repulsions associated with stretching the lipid and polymer chains. Thus, the optimal area is the one in which the lipid and polymer combined exert a repulsive interaction exactly equal to the (attractive) water-oil surface tension (see Fig. 1). As mentioned above, this limits the number of polymers that can be in the bilayer, as a large surface coverage of polymer results in a large repulsive interaction. Under these conditions, the PEG and lipid tail contributions exceed the surface tension attraction, thus breaking the aggregate. For conditions that we are interested in, it turns out that the most dominant contribution determining the area per molecule arises from the lipid tails. Actually, in most cases, neglecting the polymer contribution to determine the optimal area will give an error in the estimated area per molecule of $<2\%$.

In a recent paper, the effect of lateral expansion induced by polymer brushes on the lipid layer was taken into account to study elastic constants of polymer-grafted lipid membranes (Marsh, 2001). The area changes predicted in the range of polymer concentration of experimental interest are $<5\%$. It should be stressed, however, that for the determination of the elastic properties of the bilayers none of the contributions can be neglected, as it will be shown in the Results section.

The free energy of the aggregate from a molecular theory and the optimal packing area have now been described. The next step is to use that molecular free energy to determine the phenomenological coefficients that are presented in Eq. 5. To this end, we follow the same procedure of Szleifer et al. (1990), in which the explicit expression of the free energy from the molecular theory is differentiated with respect to curvature, lipid, and polymer asymmetry. In our case, however, we need to take derivatives up to fourth-order to obtain all the coefficients of the expansion. The results of the expansion are shown in the Appendix, with all the necessary details of how the calculation is carried out. The main result is that all the coefficients can be obtained from the knowledge of the properties of the equilibrium planar film. Therefore, the calculations, even though not trivial, become feasible for a large variety of relevant experimental accessible variables, without the need to perform calculations for each curvature and composition of lipid and polymer.

To summarize, we use the molecular theory to obtain the expansion coefficients that are necessary to determine the optimal size and structure of the spontaneously forming liposomes. Furthermore, if we now have the coefficients of the expansion we can calculate the free energy under all conditions.

In principle, we can determine the complete size distribution of the aggregates by combining the free energy of a single aggregate, Eq. 5, with a mixing term of the aggregates, in the ideal solution limit. The size distribution is then obtained by the minimization of that free energy subject to the constrain that the sum of lipids and the sum of polymers over all aggregates, weighted by the appropriate number of the aggregates, gives the total number of lipids and polymers present in solution. This will be pursued in future work.

All the calculations presented below were carried out for double tail lipid bilayers of varying length. Each lipid tail was of the form $—(CH_2)_n—CH_3$, with $11 < n < 15$. Each $—CH_2—$ group was modeled as a unit and the chains were generated using the rotational isomeric state model (Flory, 1988) with the appropriate bond length and bond angles. Each bond was allowed to have one *trans* or two *gauche* configurations. The energetic price of the *gauche* configuration was taken as 500 cal/mol. Thus, the internal energy of a configuration is given by the number of *gauche* bonds multiplied by the *gauche* energy. The volume of a $—CH_2—$ group was taken as 27 $Å^3$, while that of the $—CH_3$ was equal to 54 $Å^3$. For the lipid tails, all the possible configurations of the chains were generated and only

those that were self-avoiding were used in the calculations. For details of the chain model of the hydrocarbon tails and how the calculations are carried out, see Szleifer et al. (1986, 1990). The model PEG chains had chain lengths in the range $50 \leq N_{EG} \leq 150$. Each —CH_2—CH_2O— was taken as a unit of volume 61 Å^3 and the chains were generated using the rotational isomeric state model with the distance between EG groups taken as 3.2 Å, and the three states of each bond were taken to be isoenergetic, i.e., $\varepsilon_{intra}(\alpha) = 0$ for all α. This was the model used in Faure et al., 1998, where quantitative agreement was found for the pressure-area isotherms predicted by the theory and experimental observations of polymers containing PEG chains. We have used a sample of 1×10^6 independent self-avoiding conformations that were generated by simple sampling. For more details on the chain model, calculation details, and predictions of the theory for PEG chains, see Szleifer and Carignano (1996, 2000); Szleifer (1996, 1997a); Faure et al. (1998); and Satulovsky et al. (2000).

RESULTS AND DISCUSSION

Fig. 1 presents a schematic representation of a lipid/PEG-lipid film. It also includes a representative curve of the lateral stresses acting on the film. The relative contributions are plotted to scale. Polymer, lipid, and headgroups have repulsive interactions ($\Pi(z) > 0$), while water-oil surface tension is the attractive contribution ($\Pi(z) < 0$) that holds the system together. The larger repulsions arise from the packing of the lipid hydrophobic chains. PEG repulsions are smaller in magnitude and act at larger distances from the bilayer midplane. Both surface tension attraction and head-to-head repulsions from the lipid headgroups are assumed to act exactly at a distance corresponding to half-bilayer thickness. The magnitude of the lateral pressures has to be such that the total repulsion exactly balances the attraction, as expressed in Eq. 14.

In our previous study of spontaneous liposome formation from lipid/PEG-lipid mixtures (Szleifer et al., 1998), we used the free energy expansion up to the second order, as shown in Eq. 1. In terms of Helfrich's description of bilayer elastic constants (Helfrich, 1973), we looked at the conditions under which $K = k_b + \bar{k}/2 < 0$, where k_b is the bending elastic constant and $\bar{k}$ is the saddle-splay constant. k_b is always positive and its value can be significantly reduced by considering the relaxation of the lipids and polymers between the two monolayers (Szleifer et al., 1990; Ben-Shaul, 1995). $\bar{k}$ must be negative and larger than $2k_b$ to achieve $K < 0$. $\bar{k}$ is given by the second moment of the lateral stresses. Therefore, to maintain a tensionless membrane and obtain $K < 0$, we need to have relatively small pressures at large distances from the midplane. This was the explanation provided in our earlier work for the ability of polymer layers to induce spontaneous formation of liposomes.

Fig. 2, *top* shows K as a function of PEG loading. As the polymer loading increases, the value of the elastic constant decreases, eventually becoming negative. The different curves represent different chain lengths of PEG. The longer the polymer, the smaller the amount that it is necessary to have spontaneously forming liposomes. This has been

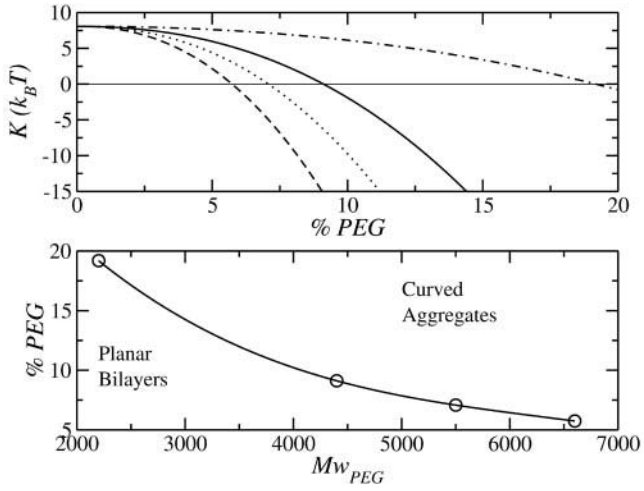

FIGURE 2 (*Top*) Elastic constant, K, as a function of the lipid-PEG loading for molecular mass of the PEG chains of 2.2 kDa (*dashed line*), 4.4 kDa (*dotted line*), 5.5 kDa (*solid line*), and 6.6 kDa (*dotted-dashed line*). The horizontal line is a guide to the eye for $K = 0$. (*Bottom*) Stability range for lamellar phases and for curved aggregates as a function of the PEG molecular mass. The line represents the percentage of PEG as a function of molecular mass at which $K = 0$. The lipid molecules have two tails each with —$(CH_2)_{15}$ —CH_3 and the lipid headgroup interactions are modeled with $\gamma = 0.12\ kT/Å^2$ and $a_h = 22.3\ Å^2$.

shown to be the result of $\bar{k}$ becoming large and negative as the chain length (and surface loading) of PEG increases, with only a small change in the value of the bending constant k_b (Szleifer et al., 1998). Fig. 2, *bottom* shows a schematic stability curve represented by the onset of the point in which K changes signs. Above the curve, spontaneous liposome formation is expected; lamellar phases are stable below it.

The results presented in Fig. 2, as well as their explanation, are essentially the same as presented in our previous work. The problem is that, while we can analyze why spontaneous liposome formation happens in terms of the bending and saddle-splay constants, two main questions remain unanswered. First, what is the size and structure of the equilibrium aggregates formed, and second, what is the physical molecular driving force for spontaneous liposome formation? To answer these questions we now turn to the predictions of the theory using the free energy expansion, including fourth-order terms in curvature and composition of lipid and PEG.

Optimal size and structure

Fig. 3 shows the free energy, including the fourth-order terms, as a function of curvature for three different loadings of PEG for chains with $N_{EG} = 100$, corresponding to PEG of $M_W = 4400$. The free energy at each curvature is the minimal free energy with respect to the PEG and lipid distribution (i.e., x_{PEG} and x_{lipid}). Namely, the calculated

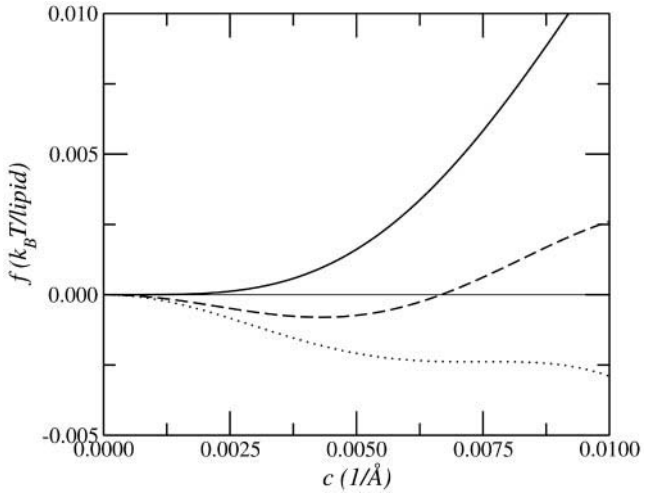

FIGURE 3 Minimum free energy as a function of curvature for a lipid/PEG-lipid bilayer containing 9.15% (*solid line*), 9.5% (*dashed line*), and 9.7% (*dotted line*) of PEG-lipid. The lipid tails are modeled as in Fig. 2 and the PEG chains have a molecular mass of 4.4 kDa.

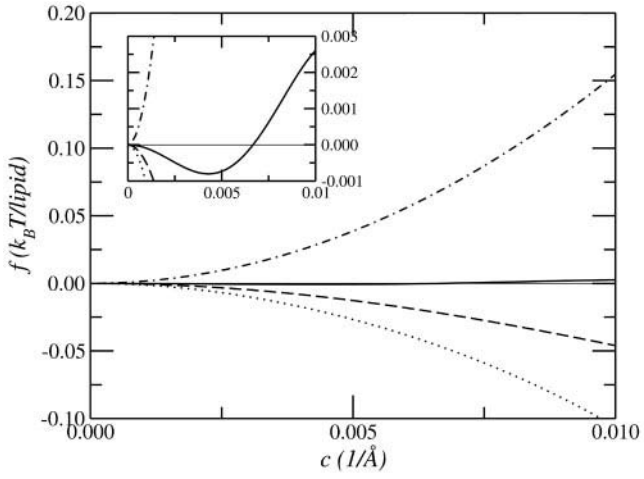

FIGURE 4 Contributions of lipid tails (f_{lipid}, *dashed line*), lipid headgroups ($f_{\text{headgroup}}$, *dotted-dashed line*), and PEG chains (f_{PEG}, *dotted line*) to the aggregate minimum free energy ($f_{\text{aggregate}}$, *solid line*) as a function of curvature. The inset presents a zoom-in of the $f_{\text{aggregate}}$ curve. Note the difference in free energy scale. The calculations correspond to the same system as Fig. 3 with PEG loading of 9.5%.

free energies are obtained by fixing the curvature and finding the optimal partition of lipid and polymer between the two monolayers. This is repeated as a function of curvature, and then the onsets of minimized free energies are plotted. The three curves show maximal free energy for the planar bilayer. This is actually already known from Fig. 2, where the second-order term becomes negative at PEG loading of 9.12%. However, Fig. 3 also provides the optimal size of the liposomes. As the loading of PEG increases, the optimal radius of the aggregate decreases. The free energy changes over the interesting range of curvatures (namely, $c < 0.01$ Å) are rather small. For example, for the intermediate loading shown the optimal aggregate has a free energy gain, as compared to the planar bilayer, of $\sim 10^{-3}$ kT per lipid molecule. This implies that the optimal aggregate will have an overall gain in free energy of ~ 20 kT as compared to the planar geometry.

Looking at the highest loading shown in Fig. 3, one can see the presence of a maximum at relatively high curvature $c \approx 0.0085$ Å^{-1}. This implies that for this polymer loading spontaneous liposomes represent a local minimum in the free energy. There is a lower minimum at even smaller radii, implying that micelles are likely the preferred structure. Note that we are using a free energy expression that should not be valid for very small aggregates, therefore we will not analyze the structure of small micelles. Nevertheless, we will discuss below why we believe these micelles will form and under what conditions.

At this point it is interesting to look at the different contributions to the free energy to see what factors induce spontaneous liposome formation. Fig. 4 shows the separate contributions to the free energy together with their sum for the intermediate loading shown in Fig. 3. The free energy contributions are evaluated for each curvature at the optimal composition, as is the case in Fig. 3. Recall that we define loading as the total amount of PEG (or polymer) in the aggregate. Composition and/or partition asymmetry refers to the partition of PEG between the two monolayers. Thus, optimal composition means, for a fixed loading, the distribution of molecules between the two monolayers that minimizes the free energy at each curvature.

The free energy of polymer and lipid chains decreases as the curvature increases. Therefore, the more curved the aggregate, the better the chains are packed. Note that this is the packing of the chains in an asymmetric bilayer as discussed below. The only positive contribution is that of the headgroups. Actually, it is the surface tension term that opposes the increase in curvature.

The three separate contributions to the free energy are relatively large. However, the sum of them results in a small free energy per molecule with a minimal free energy at finite curvature. The small free energy at the minimum and the large separate contributions to it point to the special care required in accounting for all the relevant contributions. A small variation in one of the contributions is enough to result in a large change in the optimal size or the existence of spontaneous liposomes.

To better understand the origin of each contribution to the free energy, it is best to look at the optimal partition of the polymer and lipids as a function of curvature (Fig. 5). The lipid molecules show small asymmetry as the curvature increases. The increase of the number of molecules in the outer monolayer (and consequent decrease in the inner monolayer) is the result of the larger (smaller) available

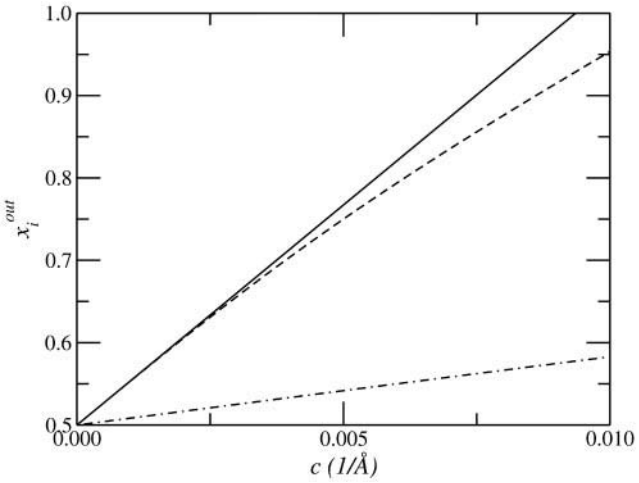

FIGURE 5 Lipid (*dotted-dashed line*) and PEG (*dashed line*) mole fraction at the outer monolayer as a function of the curvature corresponding to the equilibrium aggregate (i.e., minimum in $f_{aggregate}$) presented in Fig. 4. The mole fraction at the outer monolayer for PEG (x_{PEG}^{out}) calculated as a linear function of curvature (i.e., using Eq. 2 to first order) is also shown (*solid line*). x_{lipid}^{out} as a linear function of curvature overlaps with the curve presented for the equilibrium aggregate and it is not shown.

FIGURE 6 Schematic representation of a lipid/PEG-lipid mixture with increasing PEG loading. At low PEG loadings, the preferred structure is the planar symmetric bilayer (*A*). Intermediate loadings result in liposome formation (*B*). Micellization of the system occurs upon increasing PEG loading (*C*).

volume for packing of the chains in the outer (inner) monolayer as the curvature increases. This is optimal for the lipid tails, but it results in a high free energy cost to the surface tension term, which is proportional to the total interface area, which increases with curvature. Thus, a positive contribution to the free energy arises from the headgroup term, as shown in Fig. 4. It is interesting to note that the sum of the lipid chains and headgroup will result in an overall positive free energy, and, therefore, no spontaneous liposome formation without the inclusion of PEG.

The partition of the polymer is highly asymmetric. The results presented in Fig. 5 show that most of the polymer molecules are found in the outer monolayer. This is the result of the very large available volume spanning from the outer monolayer and the very constrained environment found in the inner part of the spherical aggregates. Additionally, for the systems studied here, PEG contributions are not coupled with any of the lipid contributions. The gain in free energy of the polymers in the outer monolayer is larger than that lost by the few remaining PEG molecules in the inner monolayer. As a consequence, an overall gain of the polymer chain contributions occurs, which serves as the driving force for spontaneous liposome formation.

The highly asymmetric partition of the polymers also explains the change in curvature of the free energy at high curvatures for the 9.7% PEG case shown in Fig. 3. As the curvature increases, the tendency of the polymers is to completely change monolayers with the optimal aggregates being eventually small spherical micelles. Our free energy expansion does not allow for an accurate description of the smaller aggregates. However, it is clear that as the asymmetry increases, the reduction in polymer free energy will overcome the surface tension increase, eventually breaking the aggregate integrity and forming micelles. The proper treatment of the micellar aggregates requires the calculation of the packing of the chains for *each* radius, as has been done for the lipid (Szleifer et al., 1986) and the polymer (Carignano and Szleifer, 1995).

Qualitatively, we can then conclude that the optimal aggregates as a function of loading are as schematically represented in Fig. 6. At low polymer loadings, planar bilayers are the optimal aggregate with a symmetric distribution of both lipids and polymers. At intermediate surface loadings, the asymmetry of the polymers, and to a smaller degree the lipids, induces the formation of optimal liposomes with finite curvature. At higher polymer loadings the tendency of PEG is to accumulate completely in the outer monolayer and, as a result, small micelles are predicted to be the optimal aggregates. Micellization of lipid/polymer-lipid systems upon increasing polymer-lipid loading has been experimentally observed (Belsito et al., 2000; Hristova et al., 1995).

The calculations presented so far use the whole fourth-order free energy expansion in terms of curvature, lipid, and PEG asymmetry. As we have shown above (see Eq. 3) the expansion up to quadratic order in curvature only requires the linear expansion terms of the composition variables. Because the determination of the fourth-order terms is rather tedious, we would like to check the validity of keeping only the linear term for the composition variables. Fig. 5 shows the linear approximation to the PEG partition asymmetry as a function of curvature. The approximation is very good up to $c \lesssim 0.0025$ Å^{-1}. For larger curvatures, the true partition of PEG is smaller than the one predicted by the linear approximation. The key question, however, is how good the linear assumption for composition will be in the total free energy prediction. To this end, Fig. 7 shows the exact free energy up to fourth-order and the free energy assuming only a linear partition variation with curvature. The approximate free energy is not very accurate for predicting the position of the minimum, and it also predicts a

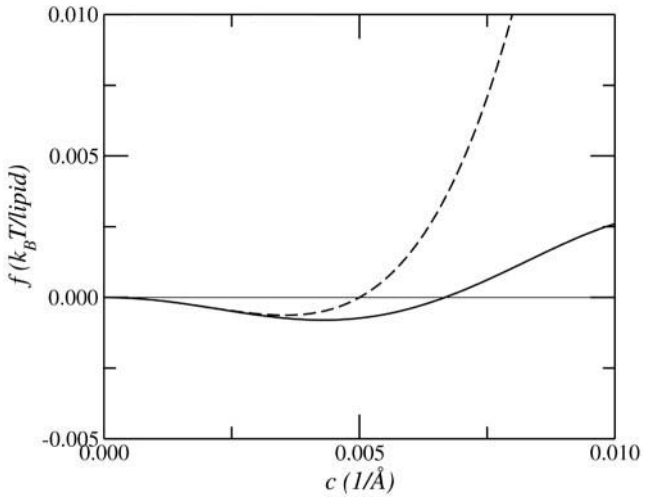

FIGURE 7 Free energy of the aggregate as a function of curvature for x_{PEG} expanded to fourth order (*solid line*) and with x_{PEG} as a linear function of c (*dotted line*) for the system presented in Fig. 4.

much stronger dependence of free energy on curvature as the curvature increases. Therefore, the linear approximation should be used only to check whether spontaneous liposome formation is possible, but to predict the structure and composition of the equilibrium aggregates, expansion to at least fourth-order is needed for all variables.

We have now determined the optimal asymmetry of lipids and PEG molecules in aggregates. The optimal size of the aggregate as a function of loading is shown in Fig. 8. The shape of the curves is the same for all PEG chain lengths. As the amount of polymer approaches the loading at which spontaneous liposome formation occurs, the optimal aggregate size shows a very sharp decrease from a

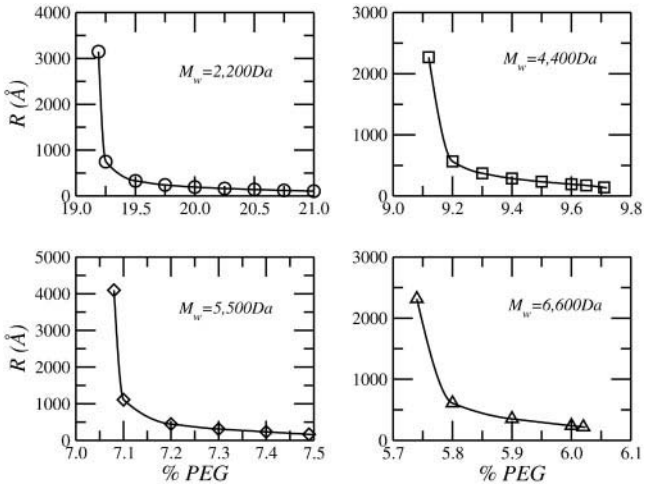

FIGURE 8 The optimal size of the aggregate as a function of PEG loading. The optimal size is the one that minimizes the total aggregates free energy. PEG molecular mass is denoted in the Figures. The lipid tails are modeled as in Fig. 2.

planar film, infinite radius to a relatively small aggregate of a few hundred angstrom radius. Note that the change in size is, in all cases, over a very narrow range of polymer loadings. This implies that control of spontaneous aggregate size will be very hard. For drug delivery applications, in particular, a desirable liposome size is of the order of 1000 Å, which for a chain with 100 segments, will be the optimal size at a loading of 9.17% PEG. However, an increase of $<0.03\%$ loading would reduce the optimal radius by half.

The very large change in optimal radius of the aggregates points to the fact that, in general, the range of phase space in which liposomes are thermodynamically stable aggregates is vary narrow. The origin of this behavior is that bilayers are the result of two frustrated monolayers that, in the case of mixtures, enable an asymmetric distribution of molecules. The resulting nonequivalent monolayers have different spontaneous curvatures and, therefore, a liposome of finite radius can form. However, the optimal packing of the polymers is that of a small micelle, as schematically shown in Fig. 6 (see also Carignano and Szleifer, 1995; Szleifer and Carignano, 1996). However, the packing of lipid molecules in small micelles is not optimal, whereas planar bilayers are. This interplay results in a range of surface loadings for which spontaneous liposomes are stable, but it is also responsible for the very sharp change of spontaneous radius as a function of PEG loading.

Proper understanding of the spontaneous size and structure of liposomes requires the knowledge of the limits in phase space where these aggregates are stable. As we have just discussed, spontaneous liposomes lie between frustrated symmetric bilayers and small micelles. The free energy curves of Fig. 3 show that a second minimum exists at very large curvatures for high PEG loadings. We construct the "phase diagram" [The true phase diagram requires the inclusions of the entropy of the solution. We refer here to "phase diagram" as the $T = 0$ case. Namely, it represents the optimal aggregates as obtained by looking at the single aggregate without solution mixing entropy and aggregate-aggregate interactions.] for stable liposomes in the following way. For each PEG-molecular weight we find the lowest loading where spontaneous liposomes may form. This composition is defined as the point where the second-order coefficient in the free energy expansion changes sign ($K = 0$). This gives us the lower bound of loading. The other limit, the maximal loading at given molecular weight, is found at the composition where the free energy is a monotonically decreasing function of curvature. Namely, it does not show a minimum in the range of curvatures that we study.

The onset of points that correspond to the upper and lower curves referred to above are represented in Fig. 9 for several polymer molecular weights. There are several interesting observations that can be made from the phase diagram. First, as previously shown (Szleifer et al., 1998), we see that spontaneous liposome formation is obtained at

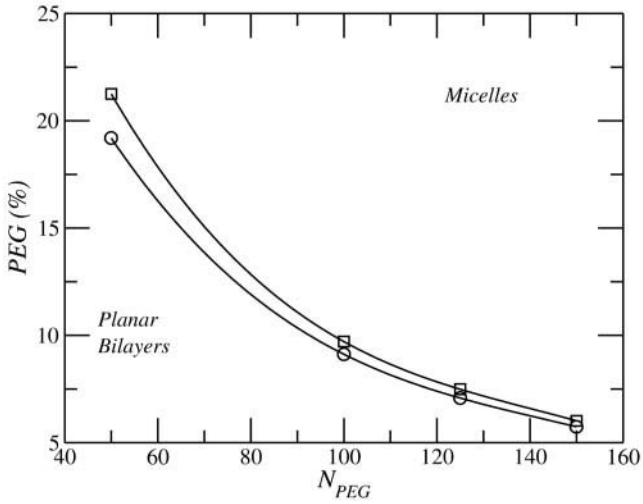

FIGURE 9 Stability range for lamellar phases, spontaneous liposomes, and micellar aggregates as a function of PEG molecular weight. The circles-line represents the percentage of PEG as a function of molecular weight at which $K = 0$. The squares-line represent the smallest percentage of PEG at which the free energy decreases monotonically with increasing curvature. The small region between the two curves is the range of stability of the spherical liposomes. The lipids are modeled as in Fig. 2.

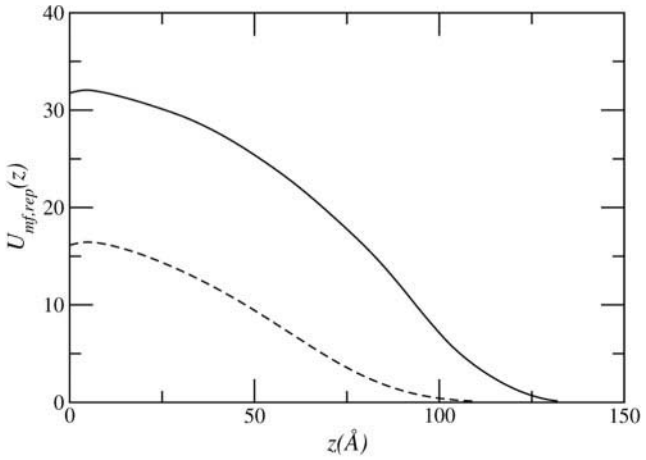

FIGURE 10 The repulsive potential of mean-force between the tethered polymer layer and model lysozyme. The dashed curve corresponds to a loading of 5% while the full line is for 10% loading. The energy is measured in thermal units, k_BT. Note that the model for the protein (and the polymers) is the same as that found to provide excellent quantitative agreement with experimental observations (McPherson et al., 1998; Satulovsky et al., 2000).

lower polymer loadings as the PEG molecular weight increases. Second, the range of loadings at which spontaneous liposomes are stable is very narrow. This is the result of small micelles becoming more stable than the large aggregates. Third, as the molecular weight increases, the range of loadings for stable liposomes decreases. This is the result of longer chains having a larger repulsion, and thus better packing, as the curvature of the grafting surface increases (Carignano and Szleifer, 1995; Szleifer and Carignano, 1996). Overall, this shows the narrow range of variables at our disposal to obtain stable spontaneous liposomes of a desired size.

We have shown above that the optimal structure of the spontaneously forming liposomes is such that there is a high asymmetry in the partition of the polymer between the inner and outer monolayers. This distribution of molecules is actually responsible for the stability of the aggregate. Moreover, there is a second very important consequence of the asymmetric distribution of polymer, namely the enhanced steric repulsion imposed by the higher polymer loading in the outer monolayer as compared to a symmetric distribution. This is very important because the main interest in PEGylated liposomes arises from the ability of the polymer molecules to increase the longevity of the aggregates in the blood stream. This enhancement is due to the ability of the polymer layer to suppress the adhesion of proteins or cells approaching the liposome surface. This is an important result because it clarifies the source of a possible contradiction. Typical loadings used in drug delivery systems are of the order of 5% PEG-5000. According to recent predictions and experimental observations of McPherson et al. (1998), this surface coverage should not be enough to effectively prevent protein adsorption if PEG was symmetrically distributed between both sides of the bilayer. The enhancement of the true loading on the outer monolayer of the liposome, however, makes the effective repulsion much larger, and thus proteins will not be able to reach the liposome surface.

To quantify the different strengths of steric barriers that result from the asymmetric distribution of polymers, we show (Fig. 10) the repulsive potential that the polymer layer presents to a model lysozyme protein. The details of the model used for the protein and the way the repulsive potential is calculated can be found elsewhere (Szleifer, 1997b). It should be stressed that these calculations provide very good agreement with experimental observations (McPherson et al., 1998). The lowest loading corresponds to the typical experimental loading of 5% PEG. The repulsive interaction, while large, is increased by more than a factor of 2 when most of the polymers are found in the outer monolayer. Thus, in a typical experimental environment in drug delivery systems, the asymmetry of the polymer induces a repulsion toward a protein-like lysozyme of >30 kT. Therefore, proteins will not be able to reach the liposome surface and the longevity of the aggregate is effectively enhanced.

At this point, it is important to stress that the repulsion calculation for lysozyme is just an example to show the very strong effect of asymmetry with respect to a small compact protein. In general, it is well known that increasing the surface coverage of polymers results in a larger steric repulsion. The secondary effect of large asymmetric distribu-

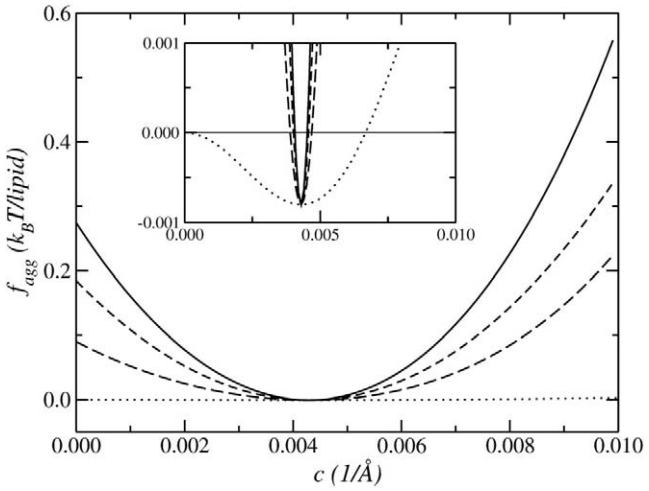

FIGURE 11 Aggregate free energy as a function of curvature for 1) equilibrium aggregates (*dotted line*); 2) aggregates with fixed molar fractions corresponding to the minimum free energy (x^{out}_{lipid} = 0.536 and x^{out}_{PEG} = 0.72, *solid line*); 3) aggregates with fixed lipid mole fraction (x^{out}_{lipid} = 0.536) and PEG mole fraction minimized at each curvature (*short-dashed line*); and 4) aggregates with fixed PEG mole fraction (x^{out}_{PEG} = 0.72) and lipid mole fraction minimized at each curvature (*long-dashed line*). The lipid/PEG-lipid system is as in Fig. 4. The inset shows a zoom around the free energy minimum.

tions of polymers as predicted here is thus a stronger repulsive barrier to particles approaching the liposome.

Stability and bending constants

The question that arises is how important the lipid and PEG asymmetry is in terms of the bilayer stability. If we fix the composition of the inner and outer monolayers of the liposome at the equilibrium values and then change the curvature without relaxing the compositions, is the free energy change going to be much larger than the one for the optimal composition at all curvatures? To answer this question we show in Fig. 11 the free energy as a function of curvature for four different ways to change the curvature from the optimal free energy. One case corresponds to the overall free energy minimum. In the second case, the PEG composition is fixed at the equilibrium value, but the lipid is allowed to change its composition as a function of curvature. The third case allows for relaxation of the polymer at fixed lipid composition and the fourth case is the one with no relaxation from the equilibrium values.

It is clear that the changes in free energy are dramatically larger for all cases where some of the compositions are kept constant. However, the relaxation of the lipids seems to be the most important in determining the elastic constants around the equilibrium structure. To quantify the effect of each degree of freedom, we can approximate the free energy around the minimum with a Helfrich-like expression, namely,

$$\frac{\delta f}{a} = \frac{1}{2} k_{\mathrm{eff}}(c - c_{\mathrm{eq}})^2 \tag{16}$$

where c_{eq} is the curvature at which the free energy is minimal and $\delta f = f - f_{eq}$. Actually, this is exactly the Helfrich free energy of a spherical bilayer expanded around the equilibrium state of the aggregate. This expression provides a quantitative way to look at the effect of the different degrees of freedom associated with deforming the equilibrium aggregate.

To get a quantitative idea of how different the observed elastic constants may be, and to see the effect of the different degrees of freedom, we have fitted the free energies shown in Fig. 11 to Eq. 16 and obtained: 1) $k^{lip,pol}_{eff} = 0.90\ k_BT$ for complete relaxation, lipids, and polymers; 2) $k^{lip}_{eff} = 41.25\ k_BT$ for relaxation of lipids but not polymers; 3) $k^{pol}_{eff} = 80.27\ k_BT$ for relaxation of polymers but not lipids; and 4) $k^{no}_{eff} = 119.20\ k_BT$ for no relaxation. There is a very sharp difference between all the different cases; however, the most pronounced difference is between the fully equilibrated elastic constant and all the other three. Because more than an order of magnitude separates the fully relaxed bending constant from the others, it is clear that it is very important to understand the type of deformation observed during the experimental determination of the aggregate's bending constants. Consider, for example, the determination of the bending constant of a bilayer by Fourier analysis of the shape fluctuations of a vesicle (Sackman and Lipowsky, 1995). The question that arises is what are the degrees of freedom that are allowed to relax when the aggregate undergoes a shape fluctuation of the kind directly probed in the experimental observations? Note that the experimental values of the bending constants on lipid bilayers of the kind modeled here is of the order of $\sim 10\ k_BT$, suggesting that these values are obtained from fluctuations that do not allow full relaxation of all the molecular degrees of freedom.

The differences in elastic constants calculated for the different modes of deformation suggest that the elastic constant that is obtained from experimental observations depends upon the way the experimental studies are carried out. For example, one way of extracting the elastic constant from experimental observations is by inversion of measured size distributions of vesicles (Jung et al., 2001). If the experimental observations are carried out in true equilibrium systems, the constant obtained is k^{free}_{eff} where all the degrees of freedom reach equilibrium at all stages. It is not clear, however, that this should also be the elastic constant that is obtained from the measurements of spontaneous shape fluctuations of vesicles. In this case, the elastic constant will depend on the time scale of the rearrangement of the molecular species within the aggregate. In most of these

cases, the experimental observations likely occur on a time scale where only partial relaxation has occurred. The different relaxations may also be responsible for the broad range of values that are reported for the bending constants in some lipid bilayers (Sackman and Lipowsky, 1995).

A second important issue regarding the elastic constants is the reference state from where they are determined. We have already used two different states for different purposes. First, we have discussed the possibility of spontaneous liposome formation from the change in sign of the elastic constant when the free energy is expanded around the planar film. This is shown in Fig. 2. However, in Fig. 11 we discuss the elastic constant around the equilibrium structure of the aggregate. The question then is whether the two cases provide different elastic constants. In the case of the free energy expansion around the planar film, the fully relaxed elastic constant is negative, while around the minimum it is (as it must be) positive. The value of the constant is -0.74 k_BT as compared to 0.90 k_BT for the value around the equilibrium state. In reality, the quadratic term obtained around the planar film should not be thought of as an elastic constant because it is not from an equilibrium state. Now, we can ask the question of how different are the elastic constants for the different types of deformation, namely $k_{\mathrm{eff}}^{\mathrm{lip}}$, $k_{\mathrm{eff}}^{\mathrm{pol}}$, and $k_{\mathrm{eff}}^{\mathrm{no}}$, determined around the symmetric planar film. There is no reason for the constants to be similar because they are obtained from two very different states and the free energy is not simply quadratic. The specific example that we describe is between the constants determined at $c = 0$; $x_{\mathrm{lip}} = 0.5$ and $x_{\mathrm{pol}} = 0.5$, and those determined at the equilibrium state $c_{\mathrm{eq}} = 0.0042$ Å^{-1}; $x_{\mathrm{lip}} = 0.536$ and $x_{\mathrm{pol}} = 0.72$. The elastic constants around the planar symmetric film are $k_{\mathrm{eff}}^{\mathrm{lip}} = 41.92$ k_BT; $k_{\mathrm{eff}}^{\mathrm{pol}} = 78.31$ k_BT, and $k_{\mathrm{eff}}^{\mathrm{no}} = 120.97$ k_BT. These values are almost identical to those determined around the minimum energy film. Therefore, the free energy cost of deforming the bilayer seems to be almost independent of the state around which it is calculated. This is surprising because the equality of the quadratic coefficient evaluated at different points is true only for exactly quadratic functions. Furthermore, for the lipid-PEG bilayers we need the fourth-order expansion on three variables to determine the equilibrium state. However, quadratic deviations from that state, keeping any variable fixed as represented by $k_{\mathrm{eff}}^{\mathrm{lip}}$, $k_{\mathrm{eff}}^{\mathrm{pol}}$, and $k_{\mathrm{eff}}^{\mathrm{no}}$, are of the same order of magnitude. This is important for practical calculations of the elastic constants because it implies that their determination around the planar film is all that is necessary.

We have discussed the effect of keeping one or two of the compositions fixed at the minimum for each curvature. However, it is very informative to also look at what happens when the curvature is kept fixed at the absolute equilibrium value and one of the compositions is varied. To this end, Fig. 12 shows the variation of free energy as a function of the lipid (polymer) fraction in the outer monolayer. In both cases, the equilibrium free energy curve is also shown. The

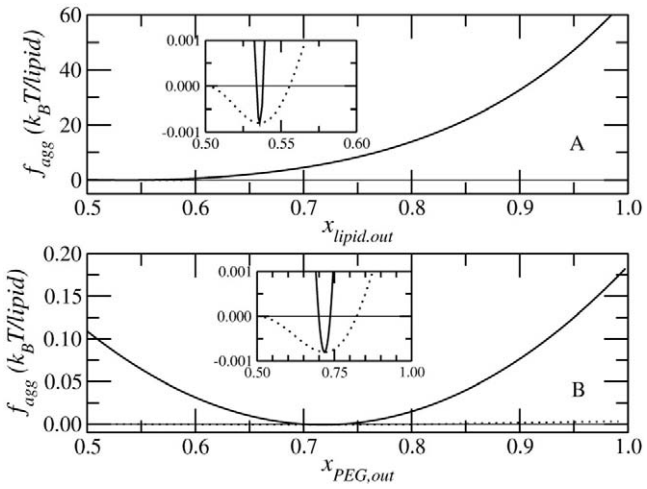

FIGURE 12 (*A*) Aggregate free energy as a function of the lipid mole fraction for 1) liposomes with fixed radius and PEG mole fraction (R = 240 Å^2 and $x_{\mathrm{PEG}}^{\mathrm{out}} = 0.72$, *solid line*) and 2) equilibrium aggregates (*dotted line*). (*B*) Aggregate free energy as a function of PEG mole fraction for 1) liposomes with fixed radius and lipid mole fraction (R = 240 Å^2 and $x_{\mathrm{lipid}}^{\mathrm{out}} = 0.536$, *solid line*) and 2) equilibrium aggregates (*dotted line*). The lipid/PEG-lipid system is the same as the one modeled in Fig. 4. The insets show a zoom around the free energy minimum.

free energy cost associated with changing the fraction of lipid molecules is very large, as was already described in relation to $k_{\mathrm{eff}}^{\mathrm{pol}}$ above. The reason is that extensive changes in the number of lipid molecules requires the breakdown of the aggregate integrity. Note that even the equilibrium value of x_{lip} at the overall free energy minimum is rather small (see also Fig. 5). The exchange of polymer molecules between the two monolayers for the equilibrium geometry of the aggregate is also costly in free energy, but not close to the degree associated with the lipid molecules. Note the different free energy scales in Fig. 12, *A* and *B*. The reason is that the polymers when inserted in the inner part of the aggregate feel a stronger repulsive field due to the geometric constraint and the neighboring polymers. However, the integrity of the aggregate remains intact.

One of the important applications of PEGylated liposomes is as stable drug carriers in vivo. The polymer coating increases the longevity in the blood stream through the introduction of a repulsive field toward approaching proteins and/or cells, as shown in the example of Fig. 10. However, once the aggregate reaches the target cell, it needs to release its contents. The question is how one can trigger this effect. We can look at the large free energy cost associated with changing the structure of the aggregate by changing its composition from the optimal composition as discussed in the last three figures. One would expect that a sharp change in the composition of the polymer in the aggregate upon reaching the target cell may lead to a breakdown of the aggregate. This can be achieved, for example, by triggering the release of the PEG molecules in the outer

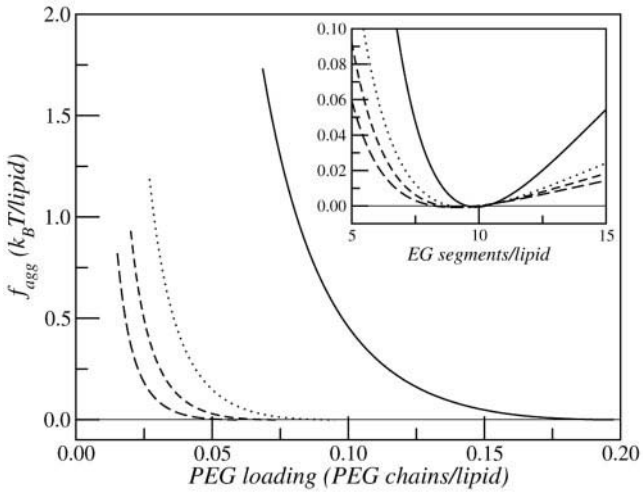

FIGURE 13 Free energy changes of lipid/PEG-lipid aggregates upon removal of the external PEG chains for PEG molecular mass of 2.2 kDa (*solid line*), 4.4 kDa (*dotted line*), 5.5 kDa (*short-dashed line*), and 6.6 kDa (*long-dashed line*). The initial aggregate has $R = 240$ Å for all the cases and the lipid mole fraction is the one that minimizes the free energy at this radius (i.e., $x_{\text{lipid}}^{\text{out}} = 0.536$) and is kept constant. The number of PEG chains within the inner monolayer is also kept constant (i.e., only the number of PEG chains in the outer monolayer changes). PEG loading is different for each molecular mass to reach an equilibrium aggregate for each case (2.2 kDa, 20% PEG-lipid; 4.4 kDa, 9.5% PEG-lipid; 5.5 kDa, 7.5% PEG-lipid; and 6.6 kDa, 6% PEG-lipid). The inset shows a zoom-in of the curves around the minimum free energy. The *x*-axis in the inset is scaled as EG segments/lipid to have all the curves within the same range. The lipids are modeled as in Fig. 2.

monolayer upon entering the cellular endosomes (Kirpotin et al., 1996; Gerasimov et al., 1999; Guo and Szoka, 2001).

We consider the following process: we start from a liposome at its equilibrium state, i.e., optimal curvature and composition of lipid and PEG on both monolayers. Now, mimicking the experimental process, we release some of the polymer molecules attached to the outer monolayer, without changing any of the other properties of the aggregate. We then calculate the free energy of the new, nonequilibrium liposome. Fig. 13 shows the free energy of this process as a function of PEG loading on the outer monolayer for a variety of different cases. There is a very large free energy cost associated with this process and, therefore, we expect that upon PEG removal from the outer monolayer, the aggregate will become thermodynamically unstable, leading to the disruption of the liposome structure and release of its content into the surrounding environment.

The free energy increase upon PEG release is a strong function of polymer molecular weight. As the molecular weight increases, the change in free energy upon removal of the polymer molecules increases. In all cases, even a partial release of the polymers is enough to increase the free energy per lipid by the thermal energy, k_BT. This implies a free energy destabilization for the whole aggregate of the order of 32,000 k_BT! The origin of this very large free energy change is associated with the large torques that suddenly appear in the aggregate. From the mechanical point of view, the optimal aggregate has zero resultant force and no torques. However, upon the release of the outer monolayer polymers, there is a non-zero torque that will have the effect of attempting to open up the inner part of the aggregate. This is due to the large repulsions between the polymers in the inner monolayer that are not balanced anymore by the outer monolayer PEG repulsions. We expect this process of destabilizing PEGylated lipids to be a very effective method for triggering drug release. Another important consideration is the time scale for aggregate breakdown. In our calculations, the free energy is minimized under constrained conditions; therefore, we cannot calculate whether kinetic barriers exist for breakdown of the aggregate. If such barriers exist, they will have the net effect of delaying the drug release process.

CONCLUSIONS

We have applied a molecular mean-field theory to study the stability and structure of spontaneous liposomes formed by mixtures of lipids and PEG-lipids. We obtained the equilibrium radius and structure of the aggregates by using a fourth-order phenomenological expansion of the free energy as a function of curvature, fraction of lipid in each monolayer, and fraction of PEG-lipid in each monolayer. The coefficients of the fourth-order expansions are determined from the molecular theory. This method enables the systematic study of many different cases without the need to determine the free energy for each possible state of the aggregate, making the calculations possible within a reasonable amount of time and keeping a great deal of molecular detail.

We find that, as the loading of polymer increases, the symmetric planar bilayer becomes unstable and a spherical aggregate becomes the optimal structure. The driving force for the formation of spherical liposomes is the gain in free energy associated with a highly *asymmetric* distribution of polymers between the two monolayers. The distribution of lipids is also asymmetric, but to a much smaller degree. By increasing the fraction of polymer molecules in the outer curved monolayer, and thus decreasing that of the inner monolayer, there is a net gain in free energy over the symmetric planar bilayer. Both the polymers and the lipid tails prefer asymmetric spherical aggregates. The only contribution to the free energy that opposes the formation of curved aggregates is the surface tension term.

Planar bilayers of lipid molecules are aggregates formed by two frustrated monolayers. The degree of frustration for lipid molecules in both monolayers is the same for symmetric bilayers. The formation of a spherical bilayer aggregate thus implies that molecules in one monolayer have a smaller degree of curvature frustration than the other. This effect promotes an asymmetric distribution of molecules so that

more molecules are less frustrated. In the case of a single component lipid of the kind studied here, this process is not enough to stabilize the asymmetric curved aggregates, therefore spontaneous liposomes are not formed. In the case of the lipid/polymer-lipid mixtures, however, the asymmetry of PEG-lipid molecules can generate a large enough gain in frustration relaxation to stabilize the spherical aggregates. The main reason for this is that changes in the distribution of lipid molecules, although favored by the lipid tails, increases the repulsive contribution of the lipid headgroups (surface tension term). Thus, the asymmetry in the number of lipids cannot be very large. The polymers, however, are not constrained in the same way, as they do not contribute to the surface tension term as the lipid headgroup do. We, therefore, see very asymmetric distributions of PEG-lipid that can stabilize the spherical mixed aggregates. Furthermore, the preferential packing of the polymers in highly curved surfaces may be large enough to drive the formation of stable small micellar aggregates. Actually, we find that the range of stable liposomes is a very narrow one, due to the tendency of the polymers to prefer the formation of small micellar aggregates with no inner monolayer attached polymers. The formation of stable liposomes, therefore, results from a delicate balance of the tendency for PEG to be packed at highly curved surfaces toward the solvent.

The asymmetric distribution of polymers in the spontaneous forming liposomes should have the added advantage that they form a better protective barrier against proteins and/or cell adsorption onto the liposome surface. This explains the increased longevity of PEGylated liposomes, even at relatively low loadings.

The elasticity of the asymmetric spherical bilayer at the optimal composition and aggregate size seems to be the same as that found in symmetric planar bilayers. This is true for all the different modes of deformation that we studied here. The stability of spherical aggregates arising from the asymmetric distribution of PEG-lipids can also be used as a basis for triggering drug delivery from long-circulating liposomes. Cleavage of PEG-lipids from the outer monolayer of spontaneous liposomes should produce aggregates that are highly unstable, even at relatively low levels of PEG desorption. This effect is more pronounced as the PEG molecular weight increases in the PEG-lipid conjugate. Liposome destabilization by PEG-lipid cleavage will occur even in kinetically stabilized aggregates, due to the very large free energy changes and the large mechanical imbalance in the cleaved aggregate. These effects have been observed in a closely related system that uses a bisvinyl ether PEG lipid conjugate (BVEP) in liposomes composed of binary mixtures of BVEP and DOPE (Boomer and coworkers, submitted for publication). Acid-catalyzed hydrolysis of BVEP in these dispersions leads to contents leakage rates that are dependent on solution pH, BVEPDOPE molar ratio, and PEG molecular weight in the BVEP conjugate. This approach is ideally suited for drug delivery applications that require long circulation for extravasation to the target tissues, followed by localized release of high concentrations of drug upon cellular uptake and endosomal acidification (Rui et al., 1998).

APPENDIX

The calculations of the elastic constants from the molecular theory require the evaluation of the derivatives of the free energy with respect to curvature, composition of lipid, and composition of polymer up to fourth order. The methodology to calculate these derivatives has been explicitly presented in previous work for lipids (Szleifer et al., 1990) and for polymers (Szleifer and Carignano, 1996). We present here a description of the main ingredients necessary to derive the equations. This is presented by showing the derivative to first order with respect to curvature. All the other derivatives needed follow along the same lines and therefore do not need to be derived explicitly. Note that the detailed derivation is only for the lipid tails and the polymer molecules. The headgroup contribution is easily obtained from the analytical derivatives of Eq. 12. Following the explanation the final equations used in the calculations are presented.

We start by writing the explicit free energy per molecule (that will contribute to the elastic constants) of the lipid and PEG contributions from Eqs. 10 and 11.

$$\begin{aligned}\frac{\beta F}{N} = &-x^{\text{in}}_{\text{PEG}} \ln Q^{\text{in}}_{\text{PEG}} - \int_{-\infty}^{-h} \beta\pi_{\text{PEG}}(z)a(z)dz \\ &- (1 - x^{\text{in}}_{\text{PEG}}) \ln Q^{\text{out}}_{\text{PEG}} - \int_{h}^{\infty} \beta\pi_{\text{PEG}}(z)a(z)dz \\ &- x^{\text{in}}_{\text{lipid}} \ln Q^{\text{in}}_{\text{lipid}} - (1 - x^{\text{in}}_{\text{lipid}}) \ln Q^{\text{out}}_{\text{lipid}} \\ &- \int_{-h}^{h} \beta\pi_{\text{lipid}}(z)a(z)dz \end{aligned} \tag{17}$$

where we have used $x^{\text{in}}_{\text{PEG}} + x^{\text{out}}_{\text{PEG}} = 1$ and $x^{\text{out}}_{\text{lipid}} + x^{\text{out}}_{\text{lipid}} = 1$. The first derivative with respect to curvature is

$$\begin{aligned}\frac{\partial(\beta F/N)}{\partial c} = &-x^{\text{in}}_{\text{PEG}} \frac{\partial \ln Q^{\text{in}}_{\text{PEG}}}{\partial c} - \frac{\partial x^{\text{in}}_{\text{PEG}}}{\partial c} \ln Q^{\text{in}}_{\text{PEG}} \\ &- \int_{-\infty}^{-h} \beta \frac{\partial \pi_{\text{PEG}}(z)}{\partial c} a(z)dz \\ &- \int_{-\infty}^{-h} \beta\pi_{\text{PEG}}(z) \frac{\partial a(z)}{\partial c} dz \\ &- (1 - x^{\text{in}}_{\text{PEG}}) \frac{\partial \ln Q^{\text{out}}_{\text{PEG}}}{\partial c} + \frac{\partial x^{\text{in}}_{\text{PEG}}}{\partial c} \ln Q^{\text{out}}_{\text{PEG}} \\ &- \int_{h}^{\infty} \beta \frac{\partial \pi_{\text{PEG}}(z)}{\partial c} a(z)dz\end{aligned}$$

$$
\begin{aligned}
&- \int_{h}^{\infty} \beta \pi_{PEG}(z) \frac{\partial a(z)}{\partial c} dz \\
&- x_{lipid}^{in} \frac{\partial \ln Q_{lipid}^{in}}{\partial c} - (1 - x_{lipid}^{in}) \frac{\partial \ln Q_{lipid}^{out}}{\partial c} \\
&- \frac{\partial x_{lipid}^{in}}{\partial c} \ln Q_{lipid}^{in} + \frac{\partial x_{lipid}^{in}}{\partial c} \ln Q_{lipid}^{out} \\
&- \int_{-h}^{h} \beta \frac{\partial \pi_{lipid}(z)}{\partial c} a(z) dz \\
&- \int_{-h}^{h} \beta \pi_{lipid}(z) \frac{\partial a(z)}{\partial c} dz \qquad (18)
\end{aligned}
$$

The next step is to calculate the derivatives of the partition functions. We show one example and the other cases follow from it. We can write

$$
\begin{aligned}
\frac{\partial \ln Q_{lipid}^{in}}{\partial c} &= \frac{1}{Q_{lipid}^{in}} \frac{\partial Q_{lipid}^{in}}{\partial c} \\
&= \frac{1}{Q_{lipid}^{in}} \frac{\partial}{\partial c} \Bigg[\sum_{\alpha} \exp(-\beta \varepsilon_{intra}(\alpha) \\
&\qquad - \int_{-h}^{h} \beta \pi_{lipid}(z) v_{lipid} n^{in}(\alpha, z) dz) \\
&= \frac{1}{Q_{lipid}^{in}} \sum_{\alpha} \exp(-\beta \varepsilon_{intra})(\alpha) \\
&\quad - \int_{-h}^{h} \beta \pi_{lipid}(z) v_{lipid} n^{in}(\alpha, z) dz) \\
&\quad \times \left(- \int_{-h}^{h} \beta \frac{\partial \pi_{lipid}(z)}{\partial c} v_{lipid} n^{in}(\alpha, z) dz \right) \\
&= - \int_{-h}^{h} \beta \frac{\partial \pi_{lipid}(z)}{\partial c} v_{lipid} \langle n^{in}(z) \rangle dz \qquad (19)
\end{aligned}
$$

Using this result and the equivalent for the other derivatives, we obtain for the first derivative with respect to the curvature

$$
\begin{aligned}
\frac{\partial (\beta F/N)}{\partial c} &= - \frac{\partial x_{PEG}^{in}}{\partial c} \ln Q_{PEG}^{in} \\
&\quad + \int_{-\infty}^{-h} (1 - \exp[-\beta \pi_{PEG}(z) v] \\
&\qquad - \beta \pi_{PEG}(z) v)(\partial a(z)/\partial c) dz \\
&\quad + \frac{\partial x_{PEG}^{in}}{\partial c} \ln Q_{PEG}^{out} + \int_{h}^{\infty} (1 \\
&\quad - \exp[-\beta \pi_{PEG}(z) v] \\
&\qquad - \beta \pi_{PEG}(z) v)(\partial a(z)/\partial c) dz \\
&\quad - \frac{\partial x_{lipid}^{in}}{\partial c} \ln \frac{Q_{lipid}^{in}}{Q_{lipid}^{out}} \\
&\quad - \int_{-h}^{h} \beta \pi_{lipid}(z) \frac{\partial a(z)}{\partial c} dz \qquad (20)
\end{aligned}
$$

When the derivative is evaluated at the planar film we obtain $(\partial(\beta F/N)/\partial c)_{c=0} = 0$, because $Q_{lipid}^{in}(c = 0) = Q_{lipid}^{out}(c = 0)$; $Q_{PEG}^{in}(c = 0) = Q_{PEG}^{out}(c = 0)$; $\partial A(z)/\partial c = A(0)z$; $\pi_{lipid}(z) = \pi_{lipid}(-z)$ and $\pi_{PEG}(z) = \pi_{PEG}(-z)$. This implies that the planar symmetric film is an extremum of the free energy as required by symmetry.

The same procedure is continued to obtain all the derivatives. Namely, for the second derivative we will differentiate Eq. 20 with respect to c. When the result is evaluated at the planar film we obtain K. The third and fourth derivatives are obtained in the same way. It is important to recall that the differentiation at all orders is done *before* evaluating at the planar film. The evaluation is done to obtain the final quantities required for the free energy expansion.

Now we have all the technical details to determine the derivatives up to fourth-order. We do not show here the step-by-step derivation because that is straightforward from the application of Eqs. 17–20.

The second-order derivatives, including the headgroup contribution, are for the curvature derivatives

$$
\begin{aligned}
f_{c^2} &= - \frac{1}{v_{lipid}} \int_{-h}^{h} \beta \pi(z) v 2a(0) z^2 dz \\
&\quad - \frac{1}{v_{lipid}} \int_{-h}^{h} 2 \frac{\partial \beta \pi(z)}{\partial c} a(0) z dz \\
&\quad - \frac{2}{v} \int_{h}^{\infty} [\exp(-\beta \pi(z) v) - 1 + \beta \pi(z) v] 2a(0) z^2 dz \\
&\quad + \frac{2}{v} \int_{h}^{\infty} \frac{\partial \beta \pi(z)}{\partial c} [\exp(-\beta \pi(z) v) - 1] 2a(0) z dz \\
&\quad + 2\gamma \left(1 + \frac{3A_h^2}{4a_{lipid}^2} \right) 2a(0) h^2, \qquad (21)
\end{aligned}
$$

where we have used the fact that the derivatives with respect to c are determined for *fixed* x_{PEG} and x_{lipid}. The second derivative with respect to the lipid asymmetry is given by

$$
f_{x_{lipid}^2} = - \int_{-h}^{h} \frac{\partial \beta \pi(z)}{\partial x_{lipid}} [\langle n_{lipid}^{in}(z) \rangle - \langle n_{lipid}^{out}(z) \rangle] dz + \frac{4\gamma A_h^2}{a_{lipid}} \qquad (22)
$$

and for the PEG asymmetry

$$f_{x^2_{PEG}} = 2r_{PEG}\int_{\infty}^{h}\frac{\partial\beta\pi(z)}{\partial x_{PEG}}\langle n_{PEG}(z)\rangle dz \qquad (23)$$

the mixed, curvature composition terms are for the lipid

$$f_{c,x_{lipid}} = -\frac{1}{v_{lipid}}\int_{-h}^{h}\frac{\partial\beta\pi(z)}{\partial x_{lipid}}2a(0)zdz - \frac{4\gamma hA_h^2}{a_{lipid}} \qquad (24)$$

and for the PEG

$$f_{c,x_{PEG}} = 2r_{PEG}\int_{h}^{\infty}\frac{\partial\beta\pi(z)}{\partial c}\langle n^{out}_{PEG}(z)\rangle dz \qquad (25)$$

All the quantities need to be evaluated at the planar symmetric film. Namely, the lateral pressures $\pi(z)$ appearing in all the expressions are those of the planar symmetric film. Note that we do not explicitly write $\pi(z)$ for lipid and for PEG. For simplicity we use just $\pi(z)$ and it is understood from the limits of the integrals whether it corresponds to the PEG or to the lipid. Also, the equations have been simplified by the fact that in the symmetric planar film z and $-z$ are equivalent.

We also have derivatives of the lateral pressures in the second derivatives, those are obtained by differentiating the constraint equations with respect to the desired variable. This has been shown in detail in earlier work for the lipids (Szleifer et al., 1990) and for polymers (Szleifer and Carignano, 1996), see below.

The fourth-order derivatives of the free energy with respect to curvature are

$$\begin{aligned}
f_{c^4} = &-\frac{6}{v}\int_h^\infty \exp(-\beta\pi(z)v)\left(\frac{\partial\beta\pi(z)}{\partial c}\right)^2 2a(0)z^2dz\\
&+\frac{6}{v}\int_h^\infty [\exp(-\beta\pi(z)v)-1]\left(\frac{\partial^2\beta\pi(z)}{\partial c^2}\right)2a(0)z^2dz\\
&-\frac{6}{v}\int_h^\infty \exp(-\beta\pi(z)v)\left(\frac{\partial\beta\pi(z)}{\partial c}\right)\left(\frac{\partial^2\beta\pi(z)}{\partial c^2}\right)2a(0)zdz\\
&+\frac{2}{v}\int_h^\infty [\exp(-\beta\pi(z)v)-1]\left(\frac{\partial^3\beta\pi(z)}{\partial c^3}\right)2a(0)zdz\\
&+\frac{2}{v}\int_h^\infty \exp(-\beta\pi(z)v)\left(\frac{\partial\beta\pi(z)}{\partial c}\right)^3 2a(0)zdz\\
&-\frac{1}{v}\int_{-h}^{h}\left(\frac{\partial^3\beta\pi(z)}{\partial c^3}\right)2a(0)zdz\\
&-\frac{3}{v}\int_{-h}^{h}\left(\frac{\partial^2\beta\pi(z)}{\partial c^2}\right)2a(0)z^2dz + 60\gamma h^4\frac{A_h^2}{a_{lipid}}
\end{aligned}$$

with respect to the lipid composition asymmetry

$$\begin{aligned}
f_{x^4_{lipid}} = &-\int_{-h}^{h}\left(\frac{\partial^3\beta\pi(z)}{\partial x^3_{lipid}}\right)[\langle n^{in}_{lipid}(z)\rangle - \langle n^{out}_{lipid}(z)\rangle]dz\\
&-2\int_{-h}^{h}\int_{-h}^{h}\left(\frac{\partial^2\beta\pi(z)}{\partial x^2_{lipid}}\right)\left(\frac{\partial\beta\pi(z')}{\partial x_{lipid}}\right)\\
&\qquad\cdot[C_2(n^{in}_{lipid}) - C_2(n^{out}_{lipid})]dz'dz\\
&-\int_{-h}^{h}\int_{-h}^{h}\left(\frac{\partial\beta\pi(z)}{\partial x_{lipid}}\right)\left(\frac{\partial^2\beta\pi(z')}{\partial x^2_{lipid}}\right)\\
&\qquad\cdot[C_2(n^{in}_{lipid}) - C_2(n^{out}_{lipid})]dz'dz\\
&-\int_{-h}^{h}\int_{-h}^{h}\int_{-h}^{h}\left(\frac{\partial\beta\pi(z'')}{\partial x_{lipid}}\right)\left(\frac{\partial\beta\pi(z')}{\partial x_{lipid}}\right)\left(\frac{\partial\beta\pi(z)}{\partial x_{lipid}}\right)\\
&\qquad\cdot[C_2(n^{in}_{lipid}) - C_3(n^{out}_{lipid})]dz''dz'dz
\end{aligned}$$

and with respect to the PEG asymmetry

$$\begin{aligned}
f_{x^4_{PEG}} = &\,2r_{PEG}\int_h^\infty\left(\frac{\partial^3\beta\pi(z)}{\partial x^3_{PEG}}\right)\langle n_{PEG}(z)\rangle dz\\
&-2r_{PEG}\int_h^\infty\int_h^\infty\left(\frac{\partial^2\beta\pi(z')}{\partial x_{PEG}}\right)\left(\frac{\partial\beta\pi(z)}{\partial x_{PEG}}\right)C_2(n_{PEG})dz'dz\\
&+4r_{PEG}\int_h^\infty\int_h^\infty\left(\frac{\partial^2\beta\pi(z)}{\partial x^2_{PEG}}\right)\left(\frac{\partial\beta\pi(z')}{\partial x_{PEG}}\right)C_2(n_{PEG})dz'dz\\
&+2r_{PEG}\int_h^\infty\int_h^\infty\int_h^\infty\left(\frac{\partial\beta\pi(z'')}{\partial x_{PEG}}\right)\left(\frac{\partial\beta\pi(z')}{\partial x_{PEG}}\right)\\
&\qquad\cdot\left(\frac{\partial\beta\pi(z)}{\partial x_{PEG}}\right)C_3(n_{PEG})dz''dz'dz
\end{aligned}$$

The mixed derivatives are

$$\begin{aligned}
f_{x^3_{lipid},c} = &-\int_{-h}^{h}\left(\frac{\partial^3\beta\pi(z)}{\partial c\partial x^2_{lipid}}\right)[\langle n^{in}_{lipid}(z)\rangle - \langle n^{out}_{lipid}(z)\rangle]dz\\
&-\int_{-h}^{h}\int_{-h}^{h}\left(\frac{\partial^2\beta\pi(z)}{\partial x^2_{lipid}}\right)\left(\frac{\partial\beta\pi(z')}{\partial c}\right)\\
&\qquad\cdot[C_2(n^{in}_{lipid}) - C_2(n^{out}_{lipid})]dz'dz\\
&-\int_{-h}^{h}\int_{-h}^{h}\left(\frac{\partial^2\beta\pi(z)}{\partial c\partial x_{lipid}}\right)
\end{aligned}$$

$$\cdot\left(\frac{\partial\beta\pi(z')}{\partial x_{\text{lipid}}}\right)[C_2(n^{\text{in}}_{\text{lipid}}) - C_2(n^{\text{out}}_{\text{lipid}})]dz'dz$$

$$-\int_{-h}^{h}\int_{-h}^{h}\left(\frac{\partial\beta\pi(z)}{\partial x_{\text{lipid}}}\right)\left(\frac{\partial^2\beta\pi(z')}{\partial c\partial x_{\text{lipid}}}\right)\cdot[C_2(n^{\text{in}}_{\text{lipid}}) - C_2(n^{\text{out}}_{\text{lipid}})]dz'dz$$

$$-\int_{-h}^{h}\int_{-h}^{h}\int_{-h}^{h}\left(\frac{\partial\beta\pi(z)}{\partial x_{\text{lipid}}}\right)\cdot\left(\frac{\partial\beta\pi(z')}{\partial x_{\text{lipid}}}\right)\left(\frac{\partial\beta\pi(z'')}{\partial c}\right)[C_3(n^{\text{in}}_{\text{lipid}}) - C_3(n^{\text{out}}_{\text{lipid}})]dz''dz'dz$$

$$f_{x^3_{\text{PEG}},c} = 2r_{\text{PEG}}\int_h^\infty\int_h^\infty\left(\frac{\partial^2\beta\pi(z')}{\partial c\partial x_{\text{PEG}}}\right)\left(\frac{\partial\beta\pi(z)}{\partial x_{\text{PEG}}}\right)C_2(n_{\text{PEG}})dz'dz$$

$$+ 2r_{\text{PEG}}\int_h^\infty\int_h^\infty\left(\frac{\partial\beta\pi(z')}{\partial x_{\text{PEG}}}\right)\cdot\left(\frac{\partial^2\beta\pi(z)}{\partial c\partial x_{\text{PEG}}}\right)C_2(n_{\text{PEG}})dz'dz$$

$$+ 2r_{\text{PEG}}\int_h^\infty\int_h^\infty\left(\frac{\partial\beta\pi(z')}{\partial c}\right)\cdot\left(\frac{\partial^2\beta\pi(z)}{\partial x^2_{\text{PEG}}}\right)C_2(n_{\text{PEG}})dz'dz$$

$$+ 2r_{\text{PEG}}\int_h^\infty\int_h^\infty\int_h^\infty\left(\frac{\partial\beta\pi(z')}{\partial x_{\text{PEG}}}\right)\cdot\left(\frac{\partial\beta\pi(z)}{\partial x_{\text{PEG}}}\right)\left(\frac{\partial\beta\pi(z'')}{\partial c}\right)C_2(n_{\text{PEG}})dz''dz'dz$$

$$+ 2r_{\text{PEG}}\int_h^\infty\left(\frac{\partial^3\beta\pi(z)}{\partial c\partial x^2_{\text{PEG}}}\right)\langle n_{\text{PEG}}(z)\rangle dz$$

$$f_{x^2_{\text{lipid}},c^2} = -\frac{1}{v_{\text{lipid}}}\int_{-h}^{h}\left(\frac{\partial^3\beta\pi(z)}{\partial c\partial x^2_{\text{lipid}}}\right)2a(0)zdz$$

$$-\frac{1}{v_{\text{lipid}}}\int_{-h}^{h}\left(\frac{\partial^2\beta\pi(z)}{\partial x^2_{\text{lipid}}}\right)2a(0)z^2dz + 24\gamma h^2\frac{A_h^2}{a_{\text{lipid}}}$$

$$f_{x^2_{\text{PEG}},c^2} = 2r_{\text{PEG}}\int_h^\infty\int_h^\infty\left(\frac{\partial^2\beta\pi(z')}{\partial c\partial x_{\text{PEG}}}\right)\left(\frac{\partial\beta\pi(z)}{\partial c}\right)C_2(n_{\text{PEG}})dz'dz$$

$$+ 2r_{\text{PEG}}\int_h^\infty\int_h^\infty\left(\frac{\partial\beta\pi(z')}{\partial c}\right)\cdot\left(\frac{\partial^2\beta\pi(z)}{\partial c\partial x_{\text{PEG}}}\right)C_2(n_{\text{PEG}})dz'dz$$

$$+ 2r_{\text{PEG}}\int_h^\infty\int_h^\infty\left(\frac{\partial\beta\pi(z')}{\partial x_{\text{PEG}}}\right)\cdot\left(\frac{\partial^2\beta\pi(z)}{\partial c^2}\right)C_2(n_{\text{PEG}})dz'dz$$

$$+ 2r_{\text{PEG}}\int_h^\infty\int_h^\infty\int_h^\infty\left(\frac{\partial\beta\pi(z')}{\partial c}\right)\left(\frac{\partial\beta\pi(z)}{\partial c}\right)\cdot\left(\frac{\partial\beta\pi(z'')}{\partial x_{\text{PEG}}}\right)C_3(n_{\text{PEG}})dz''dz'dz$$

$$+ 2r_{\text{PEG}}\int_h^\infty\left(\frac{\partial^3\beta\pi(z)}{\partial c^2\partial x_{\text{PEG}}}\right)\langle n_{\text{PEG}}(z)\rangle dz$$

$$f_{x_{\text{lipid}},c^3} = -\frac{1}{v_{\text{lipid}}}\int_{-h}^{h}\left(\frac{\partial^3\beta\pi(z)}{\partial c^2\partial x_{\text{lipid}}}\right)2a(0)zdz$$

$$-\frac{2}{v_{\text{lipid}}}\int_{-h}^{h}\left(\frac{\partial^2\beta\pi(z)}{\partial c\partial x_{\text{lipid}}}\right)2a(0)z^2dz - 48\gamma h^3\frac{A_h^2}{a_{\text{lipid}}}$$

$$f_{x_{\text{PEG}},c^3} = 2r_{\text{PEG}}\int_h^\infty\int_h^\infty\left(\frac{\partial\beta\pi(z)}{\partial c}\right)\left(\frac{\partial^2\beta\pi(z')}{\partial c^2}\right)C_2(n_{\text{PEG}})dz'dz$$

$$+ 4r_{\text{PEG}}\int_h^\infty\int_h^\infty\left(\frac{\partial\beta\pi(z')}{\partial c}\right)\cdot\left(\frac{\partial^2\beta\pi(z)}{\partial c^2}\right)C_2(n_{\text{PEG}})dz'dz$$

$$+ 2r_{\text{PEG}}\int_h^\infty\int_h^\infty\int_h^\infty\left(\frac{\partial\beta\pi(z'')}{\partial c}\right)\cdot\left(\frac{\partial\beta\pi(z')}{\partial c}\right)\left(\frac{\partial\beta\pi(z)}{\partial c}\right)C_3(n_{\text{PEG}})dz''dz'dz$$

$$+ 2r_{\text{PEG}}\int_h^\infty\left(\frac{\partial^3\beta\pi(z)}{\partial c^3}\right)\langle n_{\text{PEG}}(z)\rangle dz$$

where

$$C_2(n) = \langle n(z)\rangle\langle n(z')\rangle - \langle n(z)n(z')\rangle$$

is the intramolecular pair-correlation function and

$$C_3(n) = 2\langle n(z)\rangle\langle n(z')\rangle\langle n(z'')\rangle + \langle n(z)n(z')n(z'')\rangle - \langle n(z)\rangle\langle n(z')n(z'')\rangle - \langle n(z')\rangle\langle n(z)n(z'')\rangle - \langle n(z'')\rangle\langle n(z')n(z)\rangle$$

is the intramolecular triplet correlation function. Again, all the quantities in all the expressions are evaluated at the planar film. The only remaining unknowns are the derivatives of the first, second, and third lateral pressures with respect to the different variables. The *i*th order derivative of the lateral pressure is determined by differentiating *i* times the constraint equation. The explicit way that this is carried out has been shown for the lipids in Szleifer et al. (1990) and for polymers in Szleifer and Carignano (1996). Here are the resulting expressions needed for the derivatives with respect to curvature, the derivatives with respect to the compositions are obtained along the same lines.

The first derivative of the lateral pressure in the polymer region is obtained from

$$r_{\mathrm{PEG}}x_{\mathrm{PEG}}\int_{\mathrm{h}}^{\infty}\frac{\partial\beta\pi(z)}{\partial c}C_2(n_{\mathrm{PEG}})dz'dz - \frac{\partial\beta\pi(z)}{\partial c}\exp(-\beta\pi(z)v)\frac{a(z)}{v}dz + \frac{1}{v}(exp(-\beta\pi(z)v)-1)\frac{\partial a(z)}{\partial c}dz = 0,$$

in the lipid region

$$\frac{1}{2}\int_{-\mathrm{h}}^{\mathrm{h}}\frac{\partial\beta\pi(z')}{\partial c}[C_2(n_{\mathrm{lipid}}^{\mathrm{in}}) + C_2(n_{\mathrm{lipid}}^{\mathrm{out}})]dz'dz - \frac{1}{v}\frac{\partial a(z)}{\partial c}dz = 0 \quad (26)$$

The second derivative in the PEG region

$$r_{\mathrm{PEG}}x_{\mathrm{PEG}}\int_{\mathrm{h}}^{\infty}\frac{\partial^2\beta\pi(z')}{\partial c^2}C_2(n_{\mathrm{PEG}})dz'dz + r_{\mathrm{PEG}}x_{\mathrm{PEG}}\int_{\mathrm{h}}^{\infty}\int_{\mathrm{h}}^{\infty}\frac{\partial\beta\pi(z')}{\partial c}\frac{\partial\beta\pi(z'')}{\partial c}C_3(n_{\mathrm{PEG}})dz''dz'dz - \frac{a(z)}{v}\frac{\partial^2\beta\pi(z)}{\partial c^2}\exp(-\beta\pi(z)v)dz + \frac{a(z)}{v}\left(\frac{\partial\beta\pi(z)}{\partial c}\right)^2\exp(\beta\pi(z)v)dz - \frac{2}{v}\frac{\partial\beta\pi(z)}{\partial c}\exp(-\beta\pi(z)v)\frac{\partial a(z)}{\partial c}dz + \frac{1}{v}(\exp(-\beta\pi(z)v)-1)\frac{\partial^2 a(z)}{dz^2}dz = 0, \quad (27)$$

and in the lipid region

$$\frac{1}{2}\int_{-\mathrm{h}}^{\mathrm{h}}\frac{\partial^2\beta\pi(z')}{\partial c^2}[C_2(n_{\mathrm{lipid}}^{\mathrm{in}}) + C_2(n_{\mathrm{lipid}}^{\mathrm{out}})]dz'dz + \frac{1}{2}\int_{-\mathrm{h}}^{\mathrm{h}}\int_{-\mathrm{h}}^{\mathrm{h}}\frac{\partial\beta\pi(z')}{\partial c}\frac{\partial\beta\pi(z'')}{\partial c}\cdot[C_3(n_{\mathrm{lipid}}^{\mathrm{in}}) + C_3(n_{\mathrm{lipid}}^{\mathrm{out}})]dz''dz'dz - \frac{1}{v}\frac{\partial^2 a(z)}{\partial c^2}dz = 0 \quad (28)$$

For the third derivative in the polymer region we need to solve

$$r_{\mathrm{PEG}}x_{\mathrm{PEG}}\int_{\mathrm{h}}^{\infty}\frac{\partial^3\beta\pi(z')}{\partial c^3}C_2(n_{\mathrm{PEG}})dz'dz + 2r_{\mathrm{PEG}}x_{\mathrm{PEG}}\int_{\mathrm{h}}^{\infty}\int_{\mathrm{h}}^{\infty}\frac{\partial^2\beta\pi(z')}{\partial c^2}\frac{\partial\beta\pi(z'')}{\partial c}\cdot C_3(n_{\mathrm{PEG}})dz''dz'dz + r_{\mathrm{PEG}}x_{\mathrm{PEG}}\times\int_{\mathrm{h}}^{\infty}\int_{\mathrm{h}}^{\infty}\frac{\partial\beta\pi(z')}{\partial c}\frac{\partial^2\beta\pi(z'')}{\partial c^2}C_3(n_{\mathrm{PEG}})dz''dz'dz + r_{\mathrm{PEG}}x_{\mathrm{PEG}}\int_{\mathrm{h}}^{\infty}\int_{\mathrm{h}}^{\infty}\int_{\mathrm{h}}^{\infty}\frac{\partial\beta\pi(z')}{\partial c}\frac{\partial\beta\pi(z'')}{\partial c}\times\frac{\partial\beta\pi(z''')}{\partial c}C_4(n_{\mathrm{PEG}})dz'''dz''dz'dz - \frac{a(z)}{v}\frac{\partial^3\beta\pi(z)}{\partial c^3}\times\exp(-\beta\pi(z)v)dz - \frac{3}{v}\frac{\partial^2\beta\pi(z)}{\partial c^2}\times\exp(-\beta\pi(z)v)\frac{\partial a(z)}{\partial c}dz + \frac{3}{v}a(z)\frac{\partial^2\beta\pi(z)}{\partial c^2}\frac{\partial\beta\pi(z)}{\partial c}\exp(-\beta\pi(z)v)dz + \frac{3}{v}\left(\frac{\partial\beta\pi(z)}{\partial c}\right)^2\frac{\partial a(z)}{\partial c}\exp(-\beta\pi(z)v)dz - \frac{3}{v}\frac{\partial\beta\pi(z)}{\partial c}\frac{\partial^2 a(z)}{\partial c^2}\exp(-\beta\pi(z)v)dz - \frac{1}{v}a(z)\left(\frac{\partial\beta\pi(z)}{\partial c}\right)^3\exp(-\beta\pi(z)v)dz = 0, \quad (29)$$

and in the lipid region

$$\frac{1}{2}\int_{-h}^{h}\frac{\partial^3\beta\pi(z')}{\partial c^3}[C_2(n_{lipid}^{in})+C_2(n_{lipid}^{out})]dz'dz$$
$$+\int_{-h}^{h}\int_{-h}^{h}\frac{\partial^2\beta\pi(z')}{\partial c^2}\frac{\partial\beta\pi(z'')}{\partial c}[C_3(n_{lipid}^{in})+C_3(n_{lipid}^{out})]dz''dz'dz$$
$$+\frac{1}{2}\int_{-h}^{h}\int_{-h}^{h}\frac{\partial^2\beta\pi(z'')}{\partial c^2}\frac{\partial\beta\pi(z')}{\partial c}[C_3(n_{lipid}^{in})+C_3(n_{lipid}^{out})]dz''dz'dz$$
$$+\frac{1}{2}\int_{-h}^{h}\int_{-h}^{h}\int_{-h}^{h}\frac{\partial\beta\pi(z')}{\partial c}\frac{\partial\beta\pi(z'')}{\partial c}\frac{\partial\beta\pi(z''')}{\partial c}\times[C_4(n_{lipid}^{in})+C_4(n_{lipid}^{out})]dz'''dz''dz'dz=0 \quad (30)$$

For the third derivatives we have used

$$\begin{aligned}C_4(n)=&\,6\langle n(z)\rangle\langle n(z')\rangle\langle n(z'')\rangle\langle n(z''')\rangle\\&-\langle n(z)n(z')n(z'')n(z''')\rangle\\&+\langle n(z)n(z''')\rangle\langle n(z')n(z'')\rangle\\&+\langle n(z)n(z'')\rangle\langle n(z')n(z''')\rangle\\&+\langle n(z)n(z')\rangle\langle n(z'')n(z''')\rangle\\&-2\langle n(z)\rangle\langle n(z')\rangle\langle n(z'')n(z''')\rangle\\&-2\langle n(z)\rangle\langle n(z'')\rangle\langle n(z')n(z''')\rangle\\&-2\langle n(z)\rangle\langle n(z''')\rangle\langle n(z'')n(z')\rangle\\&-2\langle n(z'')\rangle\langle n(z')\rangle\langle n(z)n(z''')\rangle\\&-2\langle n(z''')\rangle\langle n(z')\rangle\langle n(z'')n(z)\rangle\\&-2\langle n(z'')\rangle\langle n(z''')\rangle\langle n(z)n(z')\rangle\\&+\langle n(z)\rangle\langle n(z')n(z'')n(z''')\rangle\\&+\langle n(z')\rangle\langle n(z)n(z'')n(z''')\rangle\\&+\langle n(z'')\rangle\langle n(z')n(z)n(z''')\rangle\\&+\langle n(z''')\rangle\langle n(z')n(z'')n(z)\rangle\end{aligned} \quad (31)$$

There is, in principle, a problem with the second and higher derivatives of the lateral pressures with respect to curvature for the lipid region. Because we assume that the lipid region is assumed to be dry, then we cannot keep the area and the thickness constant for curvature variations of second order and higher. This is solved by assuming that in the midplane of the bilayer lipid region the pressure is under all conditions that of liquid hydrocarbon. We have checked that this is appropriate by calculating the derivatives by straightforward variation of the curvatures and using Eqs. 28 and 30. In both cases we find that the derivatives of the free energy are predicted to be almost the same, and thus this approximation does not influence any of the predictions and conclusions shown here.

The authors thank Dr. M. Carignano for many enlightening discussions.

This work was supported by National Institutes of Health Grant GM 55266.

REFERENCES

Allen, T. M., C. Hansen, F. Martin, C. Redemann, and A. Yau-Yong. 1991. Liposomes containing synthetic lipid derivatives of poly(ethylene glycol) show prolonged circulation half-times in vivo. *Biochim. Biophys. Acta.* 1066:29–36.

Belsito, S., R. Bartucci, G. Montesano, D. Marsh, and L. Sportelli. 2000. Molecular and mesoscopic properties of hydrophilic polymer-grafted phospholipids mixed with phosphatidylcholine in aqueous dispersion: interaction of dipalmitoyl n-poly(ethylene glycol)phosphatidylethanolamine with dipalmitoylphosphatidylcholine studied by spectrophotometry and spin-label electro spin resonance. *Biophys. J.* 78:1420–1430.

Ben-Shaul, A. 1995. Structure and Dynamics of Membranes, chapter II. R. Lipowsky and E. Sackmann, editors, Elsevier, Amsterdam.

Ben-Shaul, A., I. Szleifer, and W. M. Gelbart. 1985. Chain organization and thermodynamics in micelles and bilayers. I. Theory. *J. Chem. Phys.* 83:3597–3611.

Blume, G., and G. Cevc. 1990. Liposomes for the sustained drug release in vivo. *Biochim. Biophys. Acta.* 1029:91–97.

Blume, G., and G. Cevc. 1993. Molecular mechanism of the lipid vesicle longevity in vivo. *Biochim. Biophys. Acta.* 1146:157–168.

Bradley, A. J., D. V. Devine, S. M. Ansell, J. Janzen, and D. E. Brooks. 1998. Inhibition of liposome-induced complement activation by incorporated poly(ethylene glycol)-lipids. *Arch. Biochem. Biophys.* 357: 185–194.

Carignano, M., and I. Szleifer. 1995. Structure and thermodynamic properties of end-grafted polymers on curved surfaces. *J. Chem. Phys.* 102:8662–8669.

Ceh, B., M. Winterhalter, P. M. Frederik, J. J. Vallner, and D. D. Lasic. 1997. Stealth liposomes: from theory to product. *Adv. Drug Delivery Rev.* 24:165–177.

Dan, N., and S. A. Safran. 1993. Spontaneous curvature of mixed-copolymer bilayers. *Europhys. Lett.* 21:975–980.

Ding, J., and G. Liu. 1997. Polyisoprene-*bloc*-poly(2-cinnamoylathyl methacrylate) vesicles and their aggregates. *Macromolecules.* 30: 655–657.

Discher, B. M., Y.-Y. Won, D. S. Ege, J. C.-M. Lee, F. S. Bates, D. E. Discher, and D. A. Hammer. 1999. Polymersomes: though vesicles made from diblock copolymers. *Science.* 284:1143–1146.

Faure, M. C., P. Bassereau, M. A. Carignano, I. Szleifer, Y. Gallot, and D. Andelman. 1998. Monolayers of diblock copolymer at the air-water interface: the attractive monomer-surface case. *Eur. Phys. J. B.* 3:365–375.

Flory, P. J. 1988. Statistical Mechanics of Chain Molecules. Oxford University Press, New York.

Gerasimov, O. V., J. A. Boomer, M. M. Qualls, and D. H. Thompson. 1999. Cytosolic drug delivery using pH- and light-sensitive liposomes. *Adv. Drug Delivery Rev.* 38:317–338.

Guo, X., and F. C. Szoka. 2001. Steric stabilization of fusogenic liposomes by a low pH-sensitive PEG-diortho ester-lipid conjugate. *Bioconj. Chem.* 12:291–300.

Helfrich, W. 1973. Elastic properties of lipid bilayers: theory and possible experiments. *Z. Naturforsch.* C28:693–703.

Holland, J. W., C. Hui, P. R. Cullis, and T. D. Madden. 1996. Poly(ethylene glycol)-lipid conjugates regulate the calcium-induced fusion of liposomes composed of phosphatidylethanolamine and phosphatidylserine. *Biochemistry.* 35:2618–2624.

Hristova, K., A. Kenworthy, and T. McIntosh. 1995. Effect of bilayer composition on the phase behavior of liposomal suspensions containing poly(ethylene glycol)-lipids. *Macromolecules.* 28:7693–7699.

Hristova, K., and D. Needham. 1994. The influence of polymer-grafted lipids on the physical properties of lipid bilayers: a theoretical study. *J. Colloid Interface Sci.* 168:302–314.

Israelachvili, J. 1991. Intermolecular and Surface Forces. Academic Press, London.

Joannic, R., L. Auvray, and D. D. Lasic. 1997. Monodisperse vesicles stabilized by grafted polymers. *Phys. Rev. Lett.* 78:3402–3405.

Jung, H. T., B. Coldren, J. A. Zasadzinski, D. J. Iampietro, and E. W. Kaler. 2001. The origins of stability of spontaneous vesicles. *Proc. Natl. Acad. Sci. U.S.A.* 98:1353–1356.

Kirpotin, D., K. Hong, N. Mullah, D. Papahadjopoulos, and S. Zalipsky. 1996. Liposomes with detatchable polymer coating: destabilization and fusion of dioleoylphosphatidylethanolamine vesicles triggered by cleavage of surface-grafted poly(ethylene glycol). *FEBS Lett.* 388:115–118.

Klibanov, A. L., K. Maruyama, A. M. Beckerleg, V. P. Torchilin, and L. Huang. 1991. Activity of amphipathic poly(ethylene glycol) 5000 to prolong the circulation time of liposomes depends on the liposome size and is unfavorable for immunoliposome binding to target. *Biochim. Biophys. Acta.* 1062:142.

Luo, L., and A. Eisenberg. 2001. Thermodynamic stabilization mechanism of block copolymer vesicles. *J. Am. Chem. Soc.* 123:1012–1013.

Marsh, D. 2001. Elastic constants of polymer-grafted lipid membranes. *Biophys. J.* 81:2154–2162.

McPherson, T., A. Kidane, I. Szleifer, and K. Park. 1998. Prevention of protein adsorption by tethered poly(ethylene oxide) layers: experiments and single-chain mean-field analysis. *Langmuir.* 14:176–186.

Needham, D., T. J. McIntosh, and D. D. Lasic. 1992. Repulsive interactions and mechanical stability of polymer-grafted lipid membranes. *Biochim. Biophys. Acta.* 1108:40.

Porte, G., and C. Ligure. 1995. Mixed amphiphilic bilayers: bending elasticity and formation of vesicles. *J. Chem. Phys.* 102:4290–4298.

Rui, Y., S. Wang, P. S. Low, and D. H. Thompson. 1998. Diplasmenylcholine-folate liposomes: an efficient vehicle for intracellular drug delivery. *J. Am. Chem. Soc.* 120:11213–11218.

Sackman, E., and R. Lipowsky, editors. 1995. Structure and Dynamic of Membranes. Elsevier, Amsterdam.

Safran, S. A., P. Pincus, and D. Andelman. 1990. Theory of spontaneous vesicle formation in surfactant mixtures. *Science.* 248:354–355.

Satulovsky, J., M. A. Carignano, and I. Szleifer. 2000. Kinetic and thermodynamic control of protein adsorption. *Proc. Natl. Acad. Sci. U.S.A.* 97:9037–9041.

Szleifer, I. 1996. Statistical thermodynamics of polymers near surfaces. *Curr. Opin. Colloid Interface Sci.* 1:416–423.

Szleifer, I. 1997a. Polymers and proteins: interactions at interfaces. *Curr. Opin. Solid St. Mech.* 2:337–344.

Szleifer, I. 1997b. Protein adsorption on surfaces with grafted polymers: a theoretical approach. *Biophys. J.* 72:595–612.

Szleifer, I., A. Ben-Shaul, and W. M. Gelbart. 1986. Chain statistics in micelles: effects of surface roughness and internal energy. *J. Chem. Phys.* 85:5345–5358.

Szleifer, I., and M. Carignano. 1996. Tethered polymer layers. *Adv. Chem. Phys.* 94:165–260.

Szleifer, I., and M. Carignano. 2000. Tethered polymer layers: phase transitions and reduction of protein adsorption. *Macro. Rapid Comm.* 21:423–448.

Szleifer, I., O. V. Gerasimov, and D. H. Thompson. 1998. Spontaneous liposome formulation induced by grafted poly(ethylene oxide) layers: theoretical prediction and experimental verification. *Proc. Natl. Acad. Sci. U.S.A.* 95:1032–1037.

Szleifer, I., D. Kramer, and A. Ben-Shaul. 1990. Molecular theory of curvature elasticity in surfactant films. *J. Chem. Phys.* 92:6800–6816.

Torchilin, V. P., V. G. Omelyanenko, M. I. Papisov, A. A. Bogdanov, Jr., V. S. Trubetskoy, J. N. Herron, and C. A. Gentry. 1994a. Poly(ethylene glycol) on the liposome surface: on the mechanism of polymer-coated liposome longevity. *Biochim. Biophys. Acta.* 1195:11–20.

Torchilin, V. P., M. I. Shtilman, V. S. Trubetskoy, K. Whiteman, and A. M. Milstein. 1994b. Amphiphilic vinyl polymers effectively prolong liposome circulation time in vivo. *Biochim. Biophys. Acta.* 1195:181.

Torchilin, V. P., V. S. Trubetskoy, A. M. Milshteyn, J. Canillo, G. L. Wolf, M. I. Papisov, A. A. Bogdanov, J. Narula, B. A. Khaw, and V. G. Omelyanenko. 1994c. Targeted delivery of diagnostic agents by surface-modified liposomes. *J. Controlled Release.* 28:45.

Wang, Z.-G. 1992. Curvature instability of diblock copolymer bilayers. *Macromolecules.* 25:3702–3705.